

Bounds on MAXCUT QAOA performance for $p > 1$

Jonathan Wurtz* and Peter Love

Department of Physics and Astronomy, Tufts University, Medford, Massachusetts 02155, USA

(Dated: 10/21/2020)

We obtain worst case performance guarantees for $p = 2$ and 3 QAOA for MAXCUT on uniform 3-regular graphs. Previous work by Farhi et al obtained a lower bound on the approximation ratio of 0.692 for $p = 1$. We find a lower bound of 0.7559 for $p = 2$, where worst case graphs are those with no cycles ≤ 5 . This bound holds for any 3 regular graph evaluated at particular fixed parameters. We conjecture a hierarchy for all p , where worst case graphs have with no cycles $\leq 2p + 1$. Under this conjecture, the approximation ratio is at least 0.7924 for all 3 regular graphs and $p = 3$. In addition, using a simple indistinguishability argument we find an upper bound on the worst case approximation ratio for all p , which indicates classes of graphs for which there can be no quantum advantage for at least $p < 6$.

I. INTRODUCTION

In the rapidly developing field of quantum technology, near term quantum devices [1] are the focus of much interest. Such noisy intermediate scale quantum (NISQ) devices lack error correction and have imperfect gate implementations and environmental isolation, which restrict them to implementing only low depth algorithms. Even with these constraints, can such a device display quantum advantage? One algorithm suitable for NISQ is the quantum approximate optimization algorithm (QAOA), a hybrid quantum classical combinatorial optimization algorithm [2]. In QAOA, a classical computer optimizes $2p$ angles parameterizing an ansatz wavefunction by querying a near term quantum device. This wavefunction encodes an approximate solution to some combinatorial optimization problem. For $p \rightarrow \infty$, it is known that the ansatz wavefunction encodes the exact solution, which follows from the adiabatic theorem [3]. For finite p , the picture is less clear. What p is needed to outperform the best classical algorithm? Asking such questions leads to competition between quantum and classical algorithms [4]. For example, a QAOA algorithm for E3LIN2 [5] with quantum advantage was answered by an improved classical algorithm [6], which prompted an improved QAOA version a month later without advantage [7].

One can find worst case performance guarantees for particular classes of problem instances in QAOA. Approximate solutions to a problem achieve some fraction C of the exact solution, called the approximation ratio. A worst case performance guarantee bounds this approximation ratio from below. If the minimum approximation ratio C_{\min} obtained from the quantum algorithm is larger than the value for the best classical algorithm, then the quantum algorithm has quantum advantage, as it will produce better approximate answers. It is then important to ask what this worst case performance guarantee C_{\min} is for QAOA as a function of p .

In this paper, we apply QAOA to the NP-hard graph partitioning problem of MAXCUT [8], which partitions some graph into two sets by cutting a maximum number of edges. We will find that the worst case performance

guarantee for 3-regular graphs and $p = 2$ is $C_2 \geq 0.7559$, confirming Farhi's observation and improving on his original result for $p = 1$ of $C_1 \geq 0.692$, as expected [2]. Under a conjecture that graphs with no "visible" cycles are worst case, we find $C_3 \geq 0.7924$ for $p = 3$. Additionally, we use an argument where fixed p QAOA cannot distinguish between large cycles of even and odd length to find an upper bound on expectation values, which upper bounds the minimum approximation ratio.

The paper is structured as follows. Section II reviews QAOA applied to the MAXCUT problem. Section III details how expectation values can be computed efficiently for any bounded degree graph for fixed values of p . Sections IV and V compute the worst case performance guarantee for the $p = 1$ and 2 cases. Sections VI - IX discuss some of the implications of the worst case performance, and Section X concludes with discussion and interesting future directions.

II. THE MAXCUT PROBLEM AND QAOA

The MAXCUT problem is as follows. Given a graph \mathcal{G} of vertices V and edges E , the vertices are partitioned into two sets labeled by, say, $+$ or $-$. The goal is to find the partition of vertices such that a maximal number of edges E have one vertex in each set. Restated, a solution to the MAXCUT problem separates a graph \mathcal{G} into two subgraphs by cutting the maximum number of edges.

This problem is encoded in qubits as follows. For each vertex, assign a qubit. Given vertices $\langle i \rangle$ and edges $\langle ij \rangle$ for a graph \mathcal{G} , the maximum cut is given by the maximal eigenstate of the objective function

$$\hat{C} = \sum_{\langle ij \rangle} \frac{1}{2} (1 - \hat{\sigma}_z^i \hat{\sigma}_z^j). \quad (1)$$

Each term is a clause representing an edge of the graph \mathcal{G} , with an eigenvalue of 1 if the edge is cut, and 0 if the edge is not. Because \hat{C} is made of a sum of commuting Pauli $\hat{\sigma}_z$ terms, any eigenstate is a product state, and the maximal state can be simply read out in the Z basis.

The partitioning of vertices is obtained by assigning each vertex according to a Z measurement outcome ± 1 .

One method of computing an approximate maximal state of \hat{C} is the quantum approximate optimization algorithm (QAOA) [2; 9–14]. QAOA optimizes a variational wave function by maximizing the expectation value of the objective function with respect to a set of parameters $\{\gamma\}, \{\beta\}$

$$F_{\max} = \text{MAX}_{\gamma, \beta} : F(\gamma, \beta) = \langle \gamma, \beta | \hat{C} | \gamma, \beta \rangle. \quad (2)$$

The state preparation and evaluation of the expectation value $\langle \hat{C} \rangle$ can be done on a small quantum device, while the optimization of variational parameters $\{\gamma\}, \{\beta\}$ can be performed on a classical computer. The QAOA ansatz wave function $|\gamma, \beta\rangle$ is defined as [2]

$$|\gamma, \beta\rangle = e^{-i\beta_p \hat{B}} e^{-i\gamma_p \hat{C}} (\dots) e^{-i\beta_1 \hat{B}} e^{-i\gamma_1 \hat{C}} |+\rangle \quad (3)$$

where \hat{B} , the “mixing Hamiltonian”, is defined as $\hat{B} = \sum_i \hat{\sigma}_x^i$ and $|+\rangle$ is the equally weighted superposition state or analogously the largest eigenstate of \hat{B} . Ellipses represent p iterations of unitarily evolving the wavefunction alternatively with generators \hat{C} and \hat{B} . In the limit $p \rightarrow \infty$ the optimal state $|\gamma, \beta\rangle$ approaches the exact maximal state [2].

Given an approximate wavefunction with expectation value $\langle \hat{C} \rangle$, the state can be repeatedly measured m times in the Z basis to find a bit string whose expectation value evaluates to at least $\langle \hat{C} \rangle(1 - 1/m)$ as an approximate MAXCUT solution. This is due to the phenomena of concentration, wherein the variance of expectation values is much smaller than the expectation value itself [12].

The approximation ratio for MAXCUT is

$$C(\gamma, \beta) = \frac{F(\gamma, \beta)}{C_{\max}} \quad (4)$$

where C_{\max} is the true maximum cut for a particular graph \mathcal{G} . A number in between 0 and 1 measures how close the variational state is to the exact maximal state. A larger number indicates better performance, as bit-strings from the measurement procedure will have a better MAXCUT value. If $F_{\max} = C_{\max}$ then the variational state is the exact maximal state, and the approximation ratio is 1. Note that in practice, C_{\max} may not be known, so evaluating the approximation ratio requires it to be bounded.

III. FIXED- p ALGORITHM

It was found by Farhi in 2014 [2] that for fixed graph degree ν and particular value of p , the numerical difficulty of simulating QAOA evolution grows at most doubly exponentially in p , and linearly with number of vertices N .

In the intent of fixing notation and making the problem self contained let us begin by repeating Farhi’s derivation here. The expectation value $F(\gamma, \beta)$ can be broken into individual terms for each edge $\langle ij \rangle$

$$F(\gamma, \beta) = \sum_{\langle ij \rangle} f_{\langle ij \rangle}(\gamma, \beta) \quad \text{with} \quad f_{\langle ij \rangle}(\gamma, \beta) = \frac{1}{2} \langle \gamma, \beta | 1 - \hat{\sigma}_z^i \hat{\sigma}_z^j | \gamma, \beta \rangle, \quad (5)$$

where the expectation value has been broken into a sum over individual edges. For a particular value of p , each value of $f_{\langle ij \rangle}(\gamma, \beta)$ may be computed as

$$\frac{1}{2} - \frac{1}{2} \langle + | (\dots) e^{i\gamma_p \hat{C}} e^{i\beta_p \hat{B}} \hat{\sigma}_z^i \hat{\sigma}_z^j e^{-i\beta_p \hat{B}} e^{-i\gamma_p \hat{C}} (\dots) | + \rangle \quad (6)$$

where ellipses denote the action of the other $2p - 2$ generators.

In the Heisenberg picture, this expectation value can be computed for any value of N . The first generator \hat{B} rotates each objective function clause as

$$\hat{\sigma}_z^i \hat{\sigma}_z^j \rightarrow (\cos(2\beta_p) \hat{\sigma}_z^i + \sin(2\beta_p) \hat{\sigma}_y^i) \times (\cos(2\beta_p) \hat{\sigma}_z^j + \sin(2\beta_p) \hat{\sigma}_y^j), \quad (7)$$

keeping the Heisenberg rotated operator local to the span of the two sites i, j . Terms $\hat{\sigma}_z^k \hat{\sigma}_z^l$ in the second generator \hat{C} commute and cancel unless the edges j, k overlap with i or j . In that case, the $\hat{\sigma}_y$ are rotated into $\hat{\sigma}_x$ and $\hat{\sigma}_z$ by terms $\hat{\sigma}_z^k \hat{\sigma}_z^i$, growing to a span supporting 3 sites i, j, k for terms such as $\hat{\sigma}_z^k \hat{\sigma}_y^i \hat{\sigma}_y^j$. Repeating this one layer deeper can rotate Pauli operators on k , and so forth. From this argument, it can be seen that after p steps, the operator will have a support over a subgraph with vertices at most p edges away from the initial vertices i, j .

This means given a graph \mathcal{G} and edge $\langle ij \rangle$, in order to compute a value $f_{\langle ij \rangle}(\gamma, \beta)$ one may truncate the graph to an induced subgraph only including vertices which are at most p steps away from either i or j , and the presence of the other vertices does not contribute to the expectation value. We denote such a subgraph of edge $\langle ij \rangle$ within graph \mathcal{G} to depth p as $\mathcal{G}_{\langle ij \rangle}^p$. For a fixed p and graph degree ν , there are a finite number of unique subgraphs. For 3-regular graphs, where there are exactly 3 edges per vertex, and for $p = 1$ there are 3 subgraphs, with at most 6 vertices; for $p = 2$, there are 123 subgraphs with at most 14 vertices; for $p = 3$, there are 913,088 subgraphs with at most 30 vertices. See Section IV for more details, and Table II for enumerated subgraphs for $p = 1$ and 2. We will focus on 3-regular graphs, but these results are easily generalized to other graphs with small bounded degree.

As a technical note, because only vertices within p steps of the edge $\langle ij \rangle$ need be considered to compute $f_{\langle ij \rangle}(\gamma, \beta)$, such expectation values may be efficiently calculated in the Schrödinger picture. Because a $\hat{\sigma}_z \hat{\sigma}_z$ operator only spreads to a span over the subgraph, one need

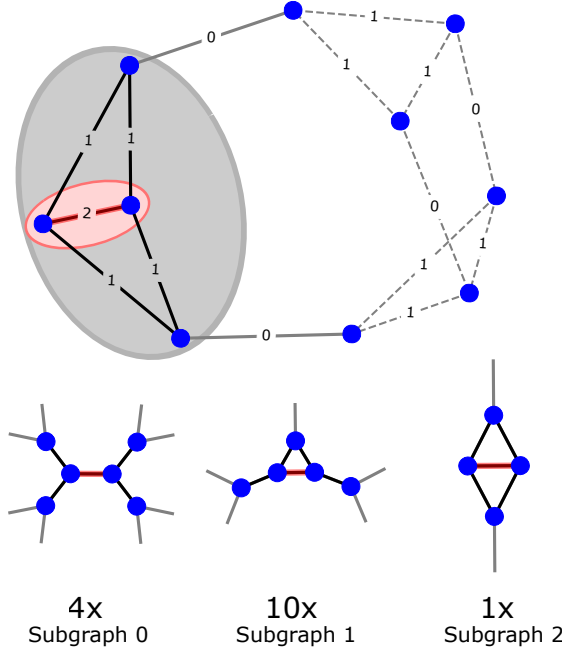


FIG. 1. An example graph with subgraph assignments for $p = 1$. Each edge (red) exists in a subgraph of edges and vertices a distance $p \leq 1$ away (grey circle). Edges within 1 step of the red edge (black) uniquely define the subgraph assignment of the edge. For this graph, there are 4 instances of subgraph 0 (“the tree”), 10 instances of subgraph 1 (“single triangle”) and one instance of subgraph 2 (“two triangles”).

only apply unitary operators over the subgraph. If the wavefunction is evolved in the Schrödinger picture under these unitaries, the state on all other sites remains an unentangled $|+\rangle$ product state, and thus one can consider the wavefunction only acting on the reduced Hilbert space of the n vertices of the subgraph. This allows computation with the order 2^n values of the wavefunction on the subgraph, instead of the order 4^n values from a general operator acting on the subgraph in the Heisenberg picture, or order 2^N values of the wavefunction on the entire graph.

The procedure for computing the expectation value $F(\gamma, \beta)$ for a particular graph \mathcal{G} of bounded degree ν and fixed p is as follows. For each edge $\langle ij \rangle$, identify the subgraph $\mathcal{G}_{\langle ij \rangle}^p$ of all edges and vertices within p steps of i and j (See Fig. 1). This defines a collection of subgraphs $\{\mathcal{G}_{\langle ij \rangle}^p | \langle ij \rangle \in \mathcal{G}\}$, one for each edge, for which each $f_{\langle ij \rangle}(\gamma, \beta)$ can be computed in parallel. This collection of subgraphs can be further decomposed by counting the number $N_\lambda(\mathcal{G})$ of each kind of subgraph λ , $\mathcal{S}_\lambda \in \{\mathcal{S}\}$ in the collection of all subgraphs of depth p , with each edge of the graph given a particular subgraph assignment $\langle ij \rangle \rightarrow \lambda$. The expectation value is then

$$F(\gamma, \beta) = \sum_{\text{subgraphs } \lambda} N_\lambda(\mathcal{G}) f_\lambda(\gamma, \beta) \quad (8)$$

where $f_\lambda(\gamma, \beta)$ is the local expectation value of the λ th subgraph.

A lower bound on the approximation ratio can be found as a fraction of two bounded terms $C_p(\mathcal{G}) = F_{\max}/C_{\max}$: a lower bound on the maximum expectation value F_{\max} and upper bound on the best MAXCUT value C_{\max} . The value F_{\max} is bounded from below by

$$F_{\max} = \max_{\gamma, \beta} F(\gamma, \beta) \geq \sum_{\lambda} N_\lambda(\mathcal{G}) f_\lambda \quad (9)$$

where $f_\lambda \equiv f_\lambda(\gamma, \beta)$ is the expectation value of an individual edge and particular subgraph λ , chosen for a particular set of values (γ, β) . The sum is guaranteed to be less than or equal to the global maximum F_{\max} , which simultaneously optimizes (γ, β) for all clauses. There is choice in the set of values for which to compute f_λ ; we use the following set of angles

$$\begin{aligned}
 p = 1 : \quad & \{\gamma_1, \beta_1\} = \{35.3^\circ, 22.5^\circ\}, \\
 p = 2 : \quad & \{\gamma_1, \beta_1, \gamma_2, \beta_2\} = \{28.0^\circ, 38.1^\circ, 51.4^\circ, 16.8^\circ\}.
 \end{aligned} \quad (10)$$

These values are one of the optima for the tree subgraph, which does not have any cycles (see Fig. 1 bottom left). For more details on this choice of angles, see Section VI.

It is hard to find the exact value for C_{\max} . However, an upper bound suffices to lower bound the approximation ratio, by considering the minimum number of uncut edges in the graph. Consider for a graph \mathcal{G} , a graph \mathcal{H} which is a collection of $N_\lambda(\mathcal{G})$ disconnected subgraphs corresponding to the subgraphs $\mathcal{G}_{\langle ij \rangle}^p$ of each edge. By brute enumeration it is simple to find the maximum fraction of edges c_λ cut per subgraph \mathcal{S}_λ . For the graph \mathcal{H} of isolated subgraphs, the global fraction of cut edges is exactly the average fraction over each subgraph, as subgraphs are disconnected.

However, multiple edges of \mathcal{H} are the same edge of \mathcal{G} . In one subgraph, an edge may be cut in a maximum configuration, while in another subgraph, no maximal configuration exists where the same edge is cut. Due to this, additional edges of \mathcal{G} may remain uncut in a globally optimal MAXCUT configuration. Thus, the sum over the MAXCUT fraction for each edges’ subgraph is an overestimate of the maximum edges cut

$$C_{\max} \leq \sum_{\lambda} N_\lambda(\mathcal{G}) c_\lambda, \quad (11)$$

where c_λ is the largest fraction of edges cut for subgraph λ .

The numerator F_{\max} is an underestimate and the denominator C_{\max} is an overestimate and so the fraction serves as a lower bound on the approximation ratio

$$C_p(\mathcal{G}) \geq \frac{\sum_{\lambda} N_\lambda(\mathcal{G}) f_\lambda}{\sum_{\lambda} N_\lambda(\mathcal{G}) c_\lambda}. \quad (12)$$

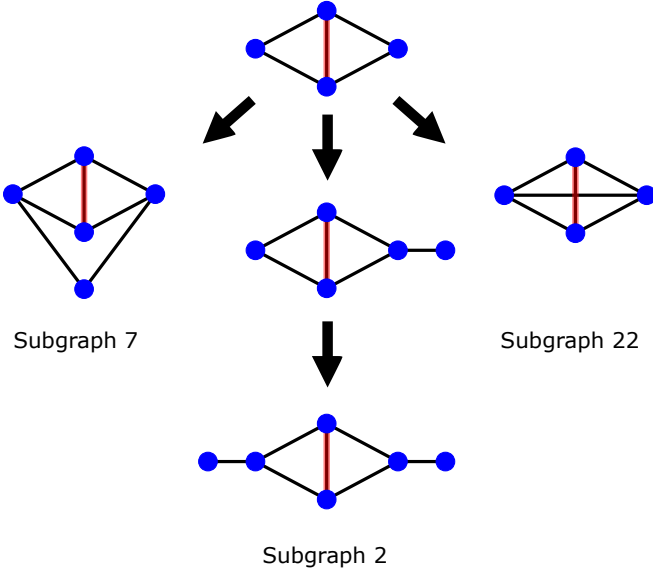


FIG. 2. Recursively constructing some $p = 2$ subgraphs. Starting from some seed $p = 1$ subgraph (top), edges are added (arrows) to vertices which do not have 3 edges already, connecting to new or existing edges. Recursion through all possibilities finds all subgraphs, up to isomorphisms. The other two $p = 1$ subgraphs have larger recursive trees, eventually finding all 123 $p = 2$ subgraphs.

Values for f_λ and c_λ for the enumerated subgraphs of $p = 1, 2$ and fixed degree $\nu = 3$ are shown in Table II, and details of the computation of f_λ are shown in appendix A.

As an example, consider the graph shown in Fig. 1. Each edge is labeled by the index of the unique subgraph identified from $\mathcal{G}_{\langle ij \rangle}^p$. For $p = 1$, there are 4 instances of subgraph 0 (“the tree”), 10 instances of subgraph 1 (“single triangle”), and 1 instance of subgraph 2 (“two triangles”). For $p = 2$ there are 6 different kinds of subgraphs. The approximation ratio for $p = 1$ becomes

$$C_1(\mathcal{G}) \geq \frac{4f_0 + 10f_1 + f_2}{4c_0 + 10c_1 + c_2}. \quad (13)$$

Using Table II, one can look up the expectation values and local MAXCUT values. The approximation ratio for this particular graph will be at least $C_1 \geq 0.759$ and $C_2 \geq 0.822$ for $p = 1$ and 2, respectively.

In this way, a lower bound on the approximation ratio of any graph can be found. This lower bound is rather pessimistic, as it chooses somewhat arbitrary angles (γ, β) . However, the particular choice of angles given by Eq. (10) appear to still have large expectation values for all subgraphs. This fact will be discussed later.

IV. SUBGRAPH GENERATION FOR FIXED P

In order to efficiently compute expectation values of graphs, one must go “in reverse” to find all possible subgraphs $\mathcal{G}_{\langle ij \rangle}^p$. This Section details the enumeration of the set of these subgraphs, denoted as $\{\mathcal{S}_\lambda\}_p$. First, find the set of all subgraphs $\{\mathcal{S}_\lambda\}_{p-1}$. For example, for $p = 1$ this is the two-vertex graph connected by an edge; for $p = 2$ these are the three $p = 1$ subgraphs, and so forth, generated recursively. Next, for each of these subgraphs, find all the exterior vertices which have less than 3 edges (see Fig. 2). Then, iterate through adding one, two, or three edges. One may add one edge connecting two vertices of the original seed subgraph (Fig. 2 Right), or add one edge connecting a vertex to a new vertex (Fig. 2 Middle). Additionally, one may add two edges connecting two vertices to a new vertex (Fig. 2 Left) or three edges connecting three vertices to a new vertex (not shown by Fig. 2). Iterating by adding these graphs to a heap, additional edges are added until all exterior vertices of the original subgraphs have three edges, and the heap is empty. This is guaranteed to find all subgraphs, as it searches through every possible permutation of new vertices connected to every combination of exterior vertices of the seed subgraph. When constructing all unique subgraphs, if a subgraph was isomorphic to an already-discovered graph, it is excluded from the heap.

Using this recursion, there were found to be 3 subgraphs for $p = 1$, 123 subgraphs for $p = 2$, and 913,088 subgraphs for $p = 3$. The $p = 1$ and $p = 2$ subgraphs are enumerated in Table II.

V. WORST CASE FOR 3-REGULAR GRAPHS

What is the worst case approximation ratio for a particular fixed value of p and given set of graphs $\{\mathcal{G}\}$? There exists some graph $\mathcal{G}_* \in \{\mathcal{G}\}$ which can be chosen maliciously such that the maximal approximation ratio $C(\mathcal{G}_*)$ is minimal in $\{\mathcal{G}\}$. This graph \mathcal{G}_* represents a problem instance for which a QAOA device with fixed p has the worst performance. Any other graph will have a larger approximation ratio and thus this worst case is a performance guarantee on QAOA.

Naïvely, finding such a graph \mathcal{G}_* is hard. The number of possible graphs is exponential in the number of vertices and we are interested in the general performance for arbitrarily large graphs, so a simple search through many graphs will not work. Because of this, a more careful approach must be taken to find lower bounds on the approximation ratio. Two methods are presented below.

The first method obtains a lower bound by finding worst case combinations of subgraphs which may or may not form a consistent graph. By considering more and more complicated combinations of subgraphs, one can get a tighter bound from below on the minimum approximation ratio. This is the approach used for the original $p = 1$ bound by Farhi [2].

The second method presents a graph hierarchy which finds that the class of graphs with no cycles less than 3 (for $p = 1$) or 5 (for $p = 2$) are worst case. This is done by finding that, given a graph \mathcal{G} , there always exists a new graph \mathcal{G}' with a smaller or equal approximation ratio. This is done by replacing edges with a subgraph to reduce the number of small cycles in the graph.

A. Lower bounds for $p = 1$

Instead of finding the exact approximation ratio of the worst case graph, one can instead *bound* the worst case approximation ratio from below, by only including subgraphs with a small approximation ratio. This is an extension of Farhi's original analysis [2]. By Eq. (12) a lower bound can be found by decomposing a graph \mathcal{G} into subgraphs of a particular set $\{\mathcal{S}_\lambda\}$. Consider the inequality

$$\frac{F}{C} \leq \frac{f'}{c'} \Leftrightarrow \frac{F}{C} \leq \frac{F + f'}{C + c'} \leq \frac{f'}{c'} \quad (14)$$

for all $f, c, F, C > 0$. In context of Eq. (12), the terms are expectation values F, f and local MAXCUT values C, c of two sets of subgraphs. One can order all subgraphs \mathcal{S}_λ by their own local approximation ratio $C_\lambda = f_\lambda/c_\lambda$ and constructively add subgraphs, starting with the subgraph with the smallest local approximation ratio.

By Eq. (14), including only the worst subgraph of a graph, or excluding the best subgraph, gives a lower bound on the global approximation ratio. Including any other subgraph with a larger local approximation ratio will only increase the value, and excluding a subgraph with a larger local approximation ratio will only decrease the value.

Taking Fig. 1 as an example graph, one can order the local approximation ratios $f_0/c_0 \leq f_2/c_2 \leq f_1/c_1$. Successive lower bounds on the approximation ratio of the graph can be found by including more and more subgraphs, eg

$$\frac{4f_0}{4c_0} \leq \frac{4f_0 + f_2}{4c_0 + c_2} \leq \frac{4f_0 + 10f_1 + f_2}{4c_0 + 10c_1 + c_2} \leq C_1(\mathcal{G}). \quad (15)$$

Adding additional subgraphs to the count gets a larger lower bound on the approximation ratio of the graph. If the graph \mathcal{G} was worst case, then this ordering results in a strict lower bound on the approximation ratio.

The worst case graph will include some number of each subgraph in its count $N_\lambda(\mathcal{G}_*)$. It is simple to iterate through the 3 possible subgraphs as enumerated in Table II to find that subgraph 0, the tree, is minimal, with $f_0/c_0 = 0.692/(5/5)$. Thus, the approximation ratio for the worst case graph \mathcal{G}_* is bounded from below by only including the minimal subgraph

$$C_1(\mathcal{G}) \geq C_{\min} \geq 0.692. \quad (16)$$

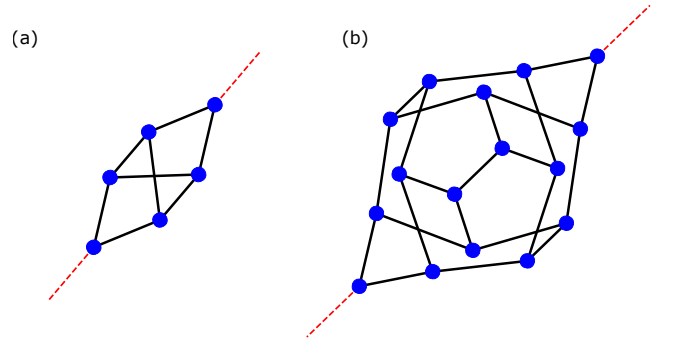


FIG. 3. Edge replacements for $p = 1$ and $p = 2$ graphs. Given an edge E , the edge is replaced by this subgraph, where red dashed indicates the original edge. The left replacement has no cycles ≤ 3 , while the right has no cycles ≤ 5 , appropriate for $p = 1$ and $p = 2$, respectively.

The analysis for the minimum approximation ratio for the $p = 1$ case ends here. This is because there are graphs which only include the tree subgraph, which have no cycles less than 4. The minimum approximation ratio $C_{\min} \leq C(\mathcal{G})$ for any graph \mathcal{G} by definition; however, $C_{\min} \leq C([\text{tree}]) = 0.692$, and so the *exact* minimum approximation ratio for $p = 1$ is this value. This is Farhi's analysis [2]: they observe that the worst graph is made only of the tree subgraph, then observe that such a graph exists. This analysis does not hold for the $p = 2$ case.

B. Graph hierarchy for $p = 1$

Before continuing to the more difficult $p = 2$ case, let us introduce a hierarchy of graphs for $p = 1$ where, heuristically, graphs with fewer small cycles have a smaller approximation ratio. We will show that, given a graph \mathcal{G} , one can always find a new graph \mathcal{G}' with $C_1(\mathcal{G}) \geq C_1(\mathcal{G}')$ unless the graph is of a specific class of graphs with no cycles of length ≤ 3 . We denote such graphs as “1-tree graphs”, which are constructed only out of the $p = 1$ tree subgraph (See Fig. 1 bottom left and Fig. 6). Similar graphs can be defined for p -tree graphs, which have no cycles of length $\leq 2p + 1$.

Given a graph with small cycles, a new graph can be found with a worse approximation ratio, which proves inductively that the graph with no small cycles is the worst case graph via recursion. Given a worst case candidate graph \mathcal{G} which is not a 1-tree, a 1-tree graph can be shown to have a smaller approximation ratio by recursion $\mathcal{G} \rightarrow \mathcal{G}' \rightarrow \mathcal{G}'' \rightarrow \dots \rightarrow \mathcal{G}_{[1\text{-tree}]} = \mathcal{G}_*$. Thus, 1-tree graphs have a lower approximation ratio than any other graph. Let us continue by proving the graph reduction $\mathcal{G} \rightarrow \mathcal{G}'$.

For a graph \mathcal{G} , choose an edge E which participates in at least one cycle of length 3. Then, replace the edge with the 6-vertex subgraph of Fig. 3a. This creates a new graph \mathcal{G}' , where the cycle of length 3 that the original

edge participated in is replaced with a new cycle of length 7. This is shown in Fig. 3. Let us prove that this new graph has a smaller approximation ratio.

When this edge is replaced, the graph is modified and so the subgraphs \mathcal{G}_{ij}^p of surrounding edges may also be modified. To prove the graph reduction, we must show that this replacement reduces the approximation ratio for all possible modifications of edges. Given some graph, the subgraph assignment of an edge is fixed by its surroundings by identifying \mathcal{G}_{ij}^p with a particular subgraph. Extending the depth of the surroundings to $2p$, one can also identify the subgraph assignment of the surrounding edges, out to a depth p , which identifies the subgraph assignment of all the edges of \mathcal{G}_{ij}^p .

The edge, and the surroundings \mathcal{G}_{ij}^{2p} which fix the subgraph assignment of adjacent edges to depth p , is called the graph environment. The set of all possible graph environments of depth p is the set of all unique combinations of subgraph assignments on the edges of all subgraphs of depth p . The six subgraph environments for $p = 1$ are shown in figure 4. For $p = 1$, there are three combinations of subgraph assignments for subgraph 0, “the tree” (Fig. 4a,b,c), two combinations of subgraph assignments for subgraph 1, “single triangle” (Fig. 4d,e), and one combination for subgraph 2, “two triangles” (Fig. 4f).

The set of graph environments is a subset of all subgraphs of depth $2p$. It is a subset because subgraphs of depth $2p$ may have cycles of length more than $2p + 1$, which the subgraph assignments of depth p cannot distinguish. Because of this fact, the set of all graph environments is equivalent to the set of subgraphs of depth $2p$, subject to the constraint of no cycles greater than $2p + 1$ in the minimum cycle basis [15].

These graph environments restrict which subgraph assignments are allowed to be adjacent. For instance, consider subgraph 2, “two triangles”. There is only one graph environment in which it is the center edge, and the adjacent edges must be assigned to subgraph 1, “one triangle”. Thus, every instance of subgraph 2 in a graph must have at least 4 instances of subgraph 1.

A subset of graph environments are the relevant graph environments, which only include edges whose subgraph assignment is modified under replacement of the center edge. For $p = 1$, there are 4 relevant graph environments, as replacing the central edge of Fig. 4a,b,c does not change the subgraph assignment of its surroundings.

Now, consider replacing a particular edge of some graph \mathcal{G} with the subgraph of figure 3a yielding a graph \mathcal{G}' . The edges of the graph can be partitioned into two sets: edges which are replaced or have their subgraph assignment modified by the replacement procedure, which are found in the relevant graph environment, and edges which are not modified. The edges which are not modified have expectation values which sum to F and local MAXCUT sum C , and the edges which are replaced or mod-

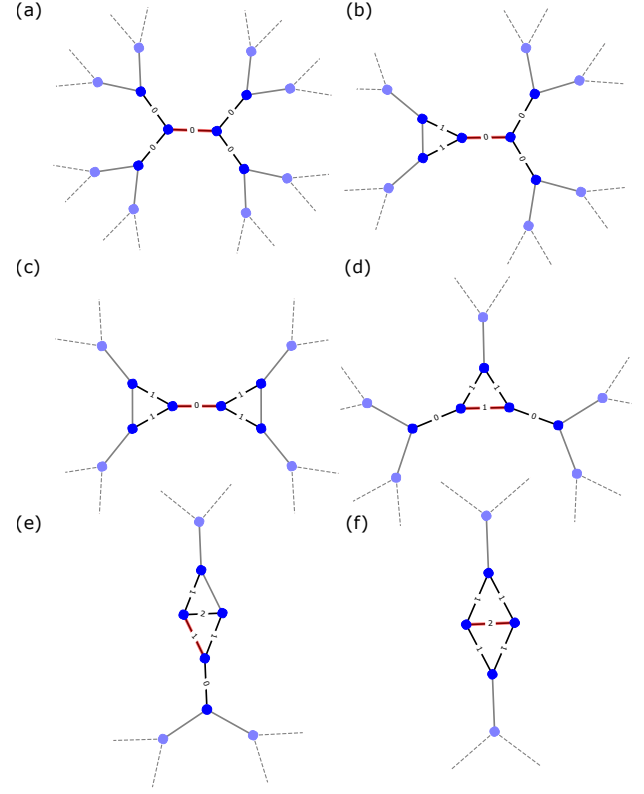


FIG. 4. The six $p = 1$ graph environments, which fix edges to particular subgraphs, as shown by edge labels. Black edges are of the center subgraph, while grey edges are choice of subgraph environment, and red is the special center edge. These graph environments mean that certain subgraphs cannot appear in isolation, and there are adjacency restrictions for certain subgraphs.

ified have expectation value sum f and local MAXCUT sum c . The replaced or modified edges have a new expectation value sum f' and local MAXCUT sum c' , which include the additional 10 edges of the replacement operation. Now, consider the following clauses and their implication

$$\begin{aligned} \mathcal{A} : \quad & \frac{F}{C} \leq \frac{f}{c}, \\ \mathcal{B} : \quad & \frac{f}{c} \geq \frac{f' - f}{c' - c}, \\ \mathcal{C} : \quad & \frac{F + f}{C + c} \geq \frac{F + f'}{C + c'}, \\ & \mathcal{A} \wedge \mathcal{B} \Rightarrow \mathcal{C}. \end{aligned} \tag{17}$$

Clause \mathcal{A} is a restriction on choice of edge E . One must choose an edge such that, if the replaced or modified edges are removed from the count of subgraphs, the approximation ratio will decrease. By Eq. (14), this choice of edge will always exist by the ordering of subgraphs.

Clause \mathcal{B} is a condition on modifying subgraph assignments of an edge and its surroundings under replacement.

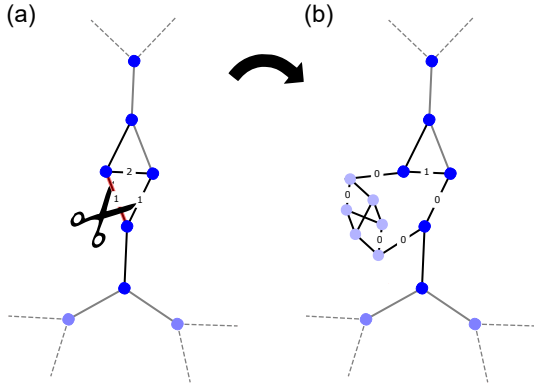


FIG. 5. An example edge replacement operation. The red center edge in some graph environment (a) is replaced with 10 edges and 6 vertices (b), removing the original size-3 cycle. The new graph with the replaced edges will have a smaller approximation ratio. Two additional edges' subgraphs (labeled) are also modified.

This can be checked for every graph environment. For $c' - c > 0$, which is the case when adding more edges under replacement, this clause is equivalent to $f/c \geq f'/c'$, that the new subgraph has a smaller local approximation ratio. Clause \mathcal{B} generalizes to other graph modifications, such as reducing a 3 cycle to a single vertex.

Clause \mathcal{C} compares the lower bound approximation ratios for the graphs \mathcal{G} and \mathcal{G}' before and after a replacement procedure. The inequality states that the approximation ratio of the new graph will be smaller. If clause \mathcal{A} and \mathcal{B} are True, then the new graph has a smaller approximation ratio, which proves the graph reduction for a particular choice of edge replacement.

As an example, consider Fig. 5, performing an edge replacement within some graph with the particular graph environment of Fig. 4e. Here, there are 3 edges whose subgraph assignments will be replaced or modified by the replacement procedure, specifically the three edges of the triangle. Two edges have a subgraph assignment of 1 (single triangle), and one has subgraph assignment of 2 (two triangles). After the procedure, there are 11 copies of subgraph 0 (the tree), and one copy of subgraph 1 (an edge of a triangle): two from the original graph environment, plus an additional 10 from the cut replacement of Fig. 3. Using Table II, one can compute

$$f = 1.911; \quad f' = 8.253; \quad c = 2.4; \quad c' = 11.8$$

It is simple to check that these values satisfy clause \mathcal{B} of Eq. (17). To prove that there always exists a graph reduction $\mathcal{G} \rightarrow \mathcal{G}'$, one can check all 4 of the relevant graph environments. It is found that clause \mathcal{B} is true for all relevant environments. Thus, it is shown that, given a graph \mathcal{G} , a new graph \mathcal{G}' can be constructed which will have a smaller or equal approximation ratio, done by replacing edges to remove cycles of length 3 in the graph. This creates a hierarchy of graphs for which graphs with fewer small cycles have a smaller approximation ratio

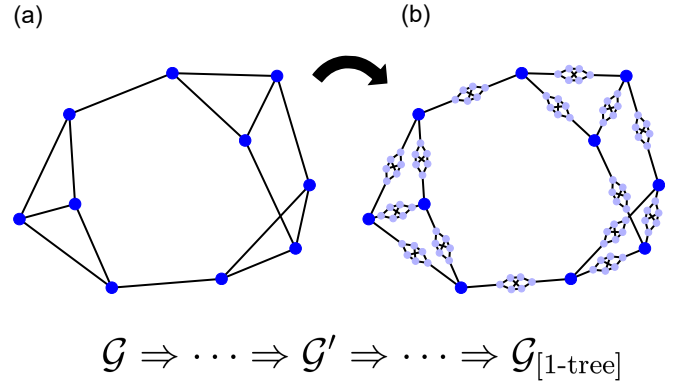


FIG. 6. An example graph reduction. Each edge of some original graph \mathcal{G} (a) is iteratively replaced with a 6 vertex subgraph, until eventually every edge is replaced to find a worst-case graph $\mathcal{G}_{[1-tree]}$ (b).

$$C(\mathcal{G}) \geq C(\mathcal{G}') \geq \dots \geq C(\mathcal{G}_{[1-tree]}) = 0.6924, \quad (18)$$

here proved for the $p = 1$ case and consistent with the lower bound and original results [2]. An example graph reduction to a 1-tree is shown in Fig. 6. This hierarchy holds for the fixed angles of Eq. (10), and so this performance guarantee holds for any graph evaluated at these fixed angles.

C. Lower bounds for $p = 2$

Finding a lower bound for $p = 2$ is more complicated, because each edge lives in a larger graph environment. These larger graph environments mean that the simple lower bound method for $p = 1$ is no longer exact. This is because the subgraph assignment of an edge constrains the subgraph assignments of neighboring edges, as there are only a finite number of graph environments. As an example, consider Fig. 4f, which is the only $p = 1$ graph environment for the two triangle subgraph 2. Any graph which includes this subgraph must by necessity also include at least 4 instances of subgraph 1 (an edge of a triangle). One cannot construct a graph out of just subgraph 2 for $p = 1$.

More generally, even though one may have some count of subgraphs N_λ , there is no guarantee that there exists a graph which has that particular count $N_\lambda \neq N_\lambda(\mathcal{G}) \forall \mathcal{G}$. A similar constraint holds for $p = 2$: neighboring and next-nearest neighboring edges may be constrained to particular configurations of subgraph assignments, due to the finite numbers of graph environments.

The worst case graph is constructed out of some count of each kind of subgraph. A lower bound on its approximation ratio can be found by only including a certain subset of its subgraphs with a small local approximation ratio, even though the subset may not have an associated graph. As a first step, one can ignore this con-

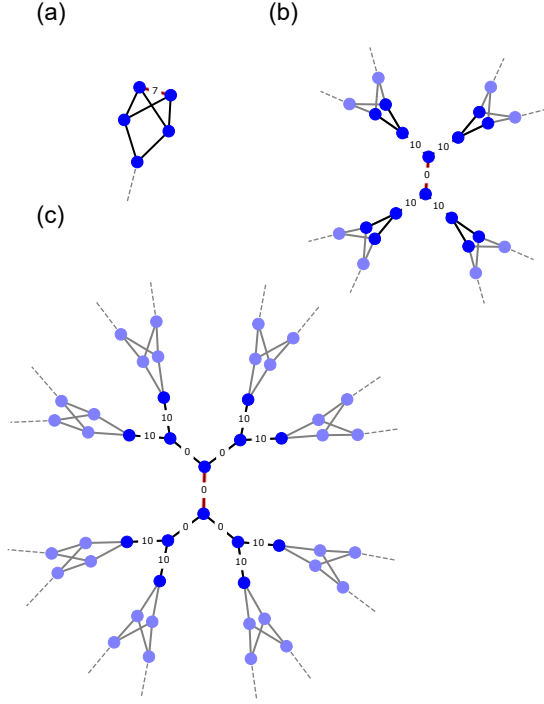


FIG. 7. The three first worst case graph environments for $p = 2$. For $N = 1$ (a), the approximation ratio is 0.4968. For $N \leq 5$ (b), it is 0.7383. For $N \leq 14$ (c), it is 0.7423. Each of these graph environments serves to find the lower bound on the approximation ratio of the worst case graph.

straint and search through the 123 unique $p = 2$ subgraphs of Table II to find the subgraph with the smallest local approximation ratio. This is shown in Fig. 7a, with $f_7/c_7 = 0.4258/(6/7) = 0.4968$. By the argument of Section V A, adding any kind of any other subgraph will increase the approximation ratio, and so this number serves as a lower bound on the minimum approximation ratio for the $p = 2$ case.

However, as is clear from inspecting this subgraph, it is impossible to construct a graph out of only this subgraph. This means that any graph which includes this subgraph will also include some combination of other subgraphs, the inclusion of which increases the approximation ratio.

Thus, this lower bound is loose, as no graph can be constructed with this approximation ratio, but any graph is guaranteed to have a larger approximation ratio. In fact, this bound is so loose that it is below the original $p = 1$ bound, which still holds for $p = 2$. This contrasts with the $p = 1$ case, where there were graphs constructed out of only the worst case subgraph and the bound was tight.

The next step in tightening this bound is to search through larger graph environments which also identify the subgraphs of the four neighboring edges to find a larger minimum approximation ratio. This graph environment is shown in Fig. 7b, and has an approximation ratio lower bounded by 0.7431, with two kinds of subgraphs. Again, it is impossible to construct a full graph

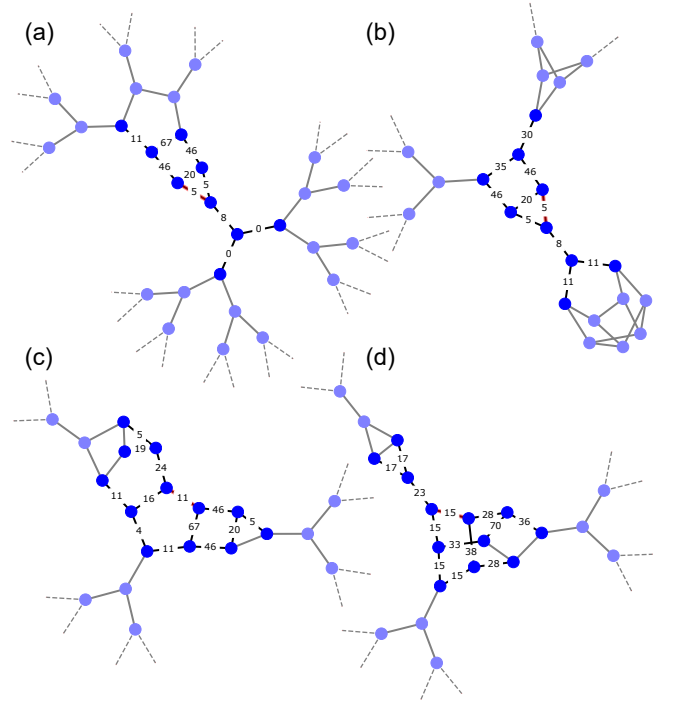


FIG. 8. Some example graph environments for $p = 2$ graphs. Subgraph edges fixed by the environment are shown by edge labels. (a,b) show two example environments for subgraph 5, while (c,d) show some example environments for subgraphs 11 and 15.

out of just this graph environment: the outer edges are not allowed to be built of those two subgraphs, and thus any graph will have a strictly larger approximation ratio.

Including graph environments one step larger identifies edges out to a depth 2 and finds the graph environment of Fig. 7c, with an approximation ratio of at least 0.7461. Beyond this limit, it becomes infeasible to find larger graph environments, due to the rapid growth in their number.

Note that, unlike the simpler $p = 1$ case, one cannot get an exact lower bound, and is instead recursively improvable by searching through larger and larger graph environments. In the next Section we consider how to approach the exact lower bound from above using the graph hierarchy.

D. Graph hierarchy for $p = 2$

Let us proceed by repeating the graph hierarchy argument of $p = 1$ for the $p = 2$ case. This case is complicated by having many more potential graph environments, because each subgraph is sensitive to a larger portion of its surroundings. Given a graph \mathcal{G} , a new graph \mathcal{G}' can be found with $C_2(\mathcal{G}) \geq C_2(\mathcal{G}')$. As in the $p = 1$ case, this is done by choosing a specific edge and replacing it with that of in Fig. 3b, which is a subgraph of 16 vertices and 25 edges.

Similarly to the $p = 1$ case, one can show that this graph reduction $\mathcal{G} \rightarrow \mathcal{G}'$ leads to a smaller approximation ratio by doing an edge replacement for every possible relevant graph environment, and checking the clauses of Eq. (17) for each. When an edge is replaced, edges up to two steps away from the replaced edge may have their subgraph assignments changed, as such subgraphs include all vertices within two steps of their center edge. Thus, one must check all $p = 2$ graph environments. These can be found via the methods of Section IV, finding all $p = 4$ subgraphs subject to the constraint that there are no cycles > 5 in the minimum cycle basis [15].

However, there are at least 30 billion $p = 2$ graph environments, which is found by estimating a combinatorial lower bound on the number of graph environments for the $p = 2$ tree subgraph. Instead, we find only the relevant graph environments. These relevant graphs are found by attempting to enumerate all relevant $p = 4$ subgraphs in parallel starting with $p = 3$ seed subgraphs, only including edges whose subgraph assignment is modified under center edge replacement. There are found to be 7058 such relevant graph environments; some examples are shown in Fig. 8.

The proof of graph reduction for $p = 2$ is as follows. For each relevant $p = 2$ graph environment, replace the special center edge and check the clauses $\mathcal{A} \wedge \mathcal{B}$ of Eq. (17). We find that clause \mathcal{B} is not satisfied for every relevant graph environment; however, there are no relevant graph environments for which \mathcal{A} (the condition on choice of edge) is False and \mathcal{B} is True. This puts a condition on choice of edge to be replaced: one must choose an edge such that \mathcal{A} is True, by only choosing edges whose inclusion increases the approximation ratio, for which \mathcal{B} will be True.

This confirms the graph hierarchy for $p = 2$. For each graph \mathcal{G} with some cycles of length ≤ 5 , choose an edge and surrounding relevant graph environment $\mathcal{G}_{(ij)}^{2p}$ which, upon removing it from the calculation of the approximation ratio, decreases the approximation ratio. This is forced by clause \mathcal{A} of Eq. (17). Upon replacing this edge with the 16-vertex edge replacement subgraph, the new graph \mathcal{G}' will be guaranteed to have a smaller (or equal) approximation ratio.

Inductively, this constructs a graph where every edge is replaced by the subgraph of Fig. 3 and has no cycles of length ≤ 5 , constructed only out of the tree subgraph. The expectation value of the tree subgraph and thus minimum approximation ratio is

$$C_2 \geq 0.7559. \quad (19)$$

where worst case graphs are 2-trees, which have no cycles ≤ 5 . This is consistent with Farhi's observation in [2].

In this Section, we have found worst case approximation ratios for $p = 1$ and 2 QAOA. Extending the original methods of Farhi, we find a recursively improvable lower bound of $C_2 \geq 0.7461$, by considering larger and larger graph environments. Unlike the $p = 1$ case, this

γ_1	β_1	γ_2	β_2
35.3°	22.5°	-	-
144.7°	22.5°	-	-
215.3°	67.5°	-	-
324.7°	67.5°	-	-
28.0°	31.8°	51.4°	16.8°
28.0°	31.8°	231.4°	73.2°
152.0°	31.8°	128.6°	73.2°
152.0°	31.8°	308.6°	16.8°
208.0°	58.2°	51.4°	73.2°
208.0°	58.2°	231.4°	16.8°
332.0°	58.2°	128.6°	16.8°
332.0°	58.2°	308.6°	73.2°

TABLE I. The angular parameters for the 4 degenerate maxima of the $p = 1$ tree subgraph, and 8 degenerate maxima of the $p = 2$ tree subgraph. The expectation value of the objective function of any graph evaluated at any of these angles is equal, and the approximation ratio is guaranteed to be above 0.6924 and 0.7559, respectively.

lower bound cannot be made exact due to the adjacency restrictions implicit in the construction of graph environments. Using a recursive graph reduction, we find that 2-tree graphs, which have no cycles ≤ 5 , are exactly worst case. For every graph which is not a 2-tree graph, a new graph can be found with a smaller approximation ratio by finding some particular edge and replacing it with a 16 vertex subgraph which has no cycles ≤ 5 . Applied recursively, this eventually turns every edge of the original graph into one of these subgraphs, which is a worst case 2-tree graph.

VI. FIXING VARIATIONAL PARAMETERS

We have shown that every graph \mathcal{G} has an approximation ratio of $C_2 \geq 0.7559$. However, this result is more general. The choice of angles (γ, β) , instead of being optimized for the particular graph, is fixed to a particular choice given by Eq. (10). This means that this performance guarantee is stronger: For *fixed* angles and any graph \mathcal{G} , the bound still holds

$$C_1(\mathcal{G}, \{35^\circ\}, \{22^\circ\}) \geq 0.6924, \quad (20)$$

$$C_2(\mathcal{G}, \{28^\circ, 31^\circ\}, \{51^\circ, 17^\circ\}) \geq 0.7559. \quad (21)$$

This particular set of angles is useful for experiments: using them with any graph guarantees a particular approximation ratio without the need of a classical optimizer back end. Additionally, we find numerically that gradient descent optimization from these angles finds the global optimum for almost every graph. It is clear why these angles were chosen: this set of angles is optimal for the worst case p -graphs. The minimum approximation ratio is found by minimizing over the set of all graphs while maximizing over angles. Any other choice of angles may have been valid, but may not have resulted in

a tight minimum approximation ratio or even have the graph hierarchy be true. In fact, this particular choice of angles generates expectation values on subgraphs which are close to the global maximum of each subgraph, which can be seen comparing rows 3 and 5 in Table II. There is no reason a priori for this to be so.

We also find that these angles are not unique. The landscape of expectation values $F(\gamma, \beta)$ is periodic modulo 2π in γ and modulo $\pi/2$ in β . This is due to $SU(2)$ and \mathbb{Z}_2 symmetry (see Appendix A for details). Within these bounds, we find 4 degenerate maxima for $p = 1$, and 8 degenerate maxima for $p = 2$. The angles for the $p = 1$ and 2 tree subgraph are shown in Table I. Further, we find that for each subgraph, the expectation value of the center edge of that subgraph is the same evaluated at each of the 8 angles of any other subgraph.

This means that for all graphs, the expectation value of the objective function will be the same for each of the 4 angular maxima of any subgraph; for example,

$$C_1(\mathcal{G}, 35^\circ, 113^\circ) = C_1(\mathcal{G}, 145^\circ, 23^\circ) \geq 0.6924 \quad (22)$$

for any graph and $p = 1$, within numerical precision, and so forth for the additional 2 angles of Table I. Any of these angles provide a good starting point for an experimentalist needing good variational parameters.

VII. CONJECTURE: p -TREE GRAPHS ARE WORST CASE

We found that removing a cycle less than length 3 or 5 results in a smaller approximation ratio for the $p = 1, 2$ cases. This naturally leads to the following conjecture:

Graph ordering conjecture: For any fixed p and graph \mathcal{G} , there exists an edge replacement with a subgraph generalized from Fig. 3 which results in a graph with a smaller approximation ratio.

In other words, there is a hierarchy of graphs, for which graphs with many small cycles less than $2p+1$ will have a better quality QAOA result than graphs with few cycles. This is shown to be true for $p = 1$ and 2 in Section VB and VD. For larger p the edge replacement must be a larger subgraph with no cycles less than $2p + 1$. This conjecture has an immediate corollary:

Large loop conjecture: The worst case graphs for fixed p are p -trees, which have no cycles less than $2p + 1$.

This conjecture is well motivated physically. When an edge is replaced, the algorithm “sees” less of the full graph, due to the fact that it only knows of relations between vertices $\leq p$ steps away [16]. This lesser knowledge of the full graph leads to worse answers, as the QAOA algorithm is then oblivious to improved solutions which “see” more of the graph. Similarly, having no “visible”

cycles means the algorithm cannot distinguish between large cycles of even vs. odd length, and thus cannot make good cut estimates which require this distinction. The worst case graph for all p would be the Bethe lattice.

A. Worst case approximation ratio for $p = 3$

Under the large loop conjecture, worst case graphs for $p = 3$ are 3-trees, with no cycles ≤ 7 and constructed only out of the 30-vertex tree subgraph, which has no loops. Using the same methods for the $p = 1$ and 2 case it is possible to compute the expectation value f_0 for this subgraph, which is thus the worst case performance guarantee for $p = 3$ under the large loop conjecture. This subgraph has 30 vertices with a Hilbert space dimension of 2^{30} . Using the symmetries of the tree subgraph, this can be reduced to a dimension of $1,631,721 \approx 2^{20.6}$, with an additional factor of $1/2$ due to spin flip symmetry (see Appendix A for details). Optimization of angles using the methods of Appendix A finds

$$C_3 \geq 0.7924 \quad (23)$$

under the large loop conjecture that 3-tree graphs are worst case for $p = 3$. In principle, this bound can be made rigorous by searching through every possible $p = 3$ graph environment and checking the inequalities of Eq. (17) for each. However there are 913,088 unique $p = 3$ graphs and a much larger number of graph environments, which must extend up to 6 steps away from the replaced edge. While in principle possible as the task is extremely parallelizable, we leave this challenging calculation to future work.

VIII. COMPARISON TO CLASSICAL ALGORITHMS

Here we compare performance bounds to the best classical algorithms. The most naïve classical algorithm is a random guess; it is simple to see that this cuts on average half the edges and so has an approximation ratio of at least 0.5 [17]. It is known that calculating a cut with approximation ratio $\geq 16/17 \approx 0.9412$ is NP-Hard [18]. The algorithm of Goemans and Williamson [19] gives an approximation ratio of at least 0.8786 using semidefinite programming, and holds for any graph. For particular subsets of graphs this approximation ratio can be higher; for example, planar graphs can be solved efficiently in polynomial time [20]. 3-regular graphs, which are the subject of this paper, have a lower bound of at least 0.9326 [21], also using semidefinite programming.

Even comparing to the general Goemans-Williamson algorithm, $p = 2$ QAOA does not achieve quantum advantage, as $0.7559 < 0.8786$. This does not discount the possibility that QAOA has better performance on a subset of graphs than any classical algorithm on the same

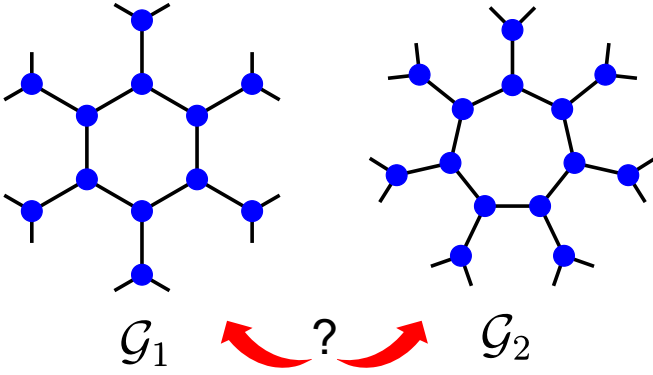


FIG. 9. $p = 2$ QAOA cannot distinguish between a tiling of hexagons (\mathcal{G}_1) or heptagons (\mathcal{G}_2), as both are constructed only from the tree subgraph. Graph \mathcal{G}_1 has a partition which cuts every edge, while graph \mathcal{G}_2 has at least one uncut edge per heptagon due to the odd length cycles. This puts upper bounds on the expectation value of the tree graph, and thus the minimum approximation ratio. This generalizes for all p and graph connectivity ν .

subset. Finding such subsets of graphs is challenging for two reasons. First, for a particular subset of graphs there may exist some classical algorithm improving on the Goemans Williamson bound, as for planar graphs or 3-regular graphs, but finding such a specialized algorithm may be nontrivial. Second, the analysis of the subgraph structure of Table II dictates the subset of allowed graphs. By the graph ordering conjecture, graphs with many cycles will have a better approximation ratios and thus have the most potential for finding instances with quantum advantage. Finding such subsets is beyond the scope of this paper.

It is a curious fact that while the classical algorithms of this paper might be able to *find* MAXCUT instances which have quantum advantage, it may not be possible to *solve* those instances classically. This is because sampling bit-strings from a QAOA wavefunction is in complexity class #P, and having such an algorithm would collapse the polynomial hierarchy at the third level [22].

IX. UPPER BOUNDS ON MINIMUM APPROXIMATION RATIO

While computing the minimum approximation ratio for $p > 3$ is challenging, it is reasonable to ask how the minimum approximation ratio behaves with p . As $p \rightarrow \infty$, the approximation ratio approaches 1 in accordance with the adiabatic theorem [2]. How does it do so? One way to compute this behavior is to bound the minimum approximation ratio from above: for a particular p , it can be *at most* some value.

One way of finding such a bound is to consider pairs of graphs which are indistinguishable under some fixed p QAOA. First, construct a bipartite graph \mathcal{G}_1 as a tiling of q -gons with cycles of length $q = 2p + 2$. For example,

for $p = 1$ this is a square ladder, while for $p = 2$ this is a hexagonal honeycomb lattice (see Fig. 9). Because all cycles are of even length, it is simple to find a partition which cuts every edge, so that $C_{\max} = n_{\text{edges}}$.

Next, construct a graph \mathcal{G}_2 , which is a tiling of q -gons with cycles of length $q = 2p + 3$. As an example, for $p = 1$ or 2 this can be seen as pentagons or heptagons (non-metrically) tiled on some curved surface (see Fig. 9). For N q -gons, there are $Nq/2$ edges. Because the cycles are of odd length, at least one edge per q -gon must remain uncut. Each edge is shared by two q -gons and so for N q -gons there are at least $N/2$ uncut edges and $C_{\max} = N(2p + 2)/2$ cut edges.

For both graphs, there are no cycles of length $\leq 2p + 1$, which means only the tree subgraph contributes to the expectation value. Critically, the tree graph cannot distinguish between the two graphs, even though they have different MAXCUT values. Consider

$$C(\mathcal{G}_1) = \frac{n_{\text{edges}} f_0}{C_{\max}} = f_0, \quad (24)$$

the approximation ratio of the bipartite graph \mathcal{G}_1 is simply the expectation value of the tree graph, as every edge is cut. By definition, $C_{\min} \leq C(\mathcal{G}_1)$. One may also compute the approximation ratio of \mathcal{G}_2 , which is bounded from above by 1.

$$C(\mathcal{G}_2) = \frac{n_{\text{edges}} f_0}{C_{\max}} = \frac{(2p + 3) f_0}{(2p + 2)} \leq 1. \quad (25)$$

This bound from above puts an upper bound on the expectation value f_0 . In combination, Eq. (24) gives an upper bound on the minimum approximation ratio

$$C_{\min} \leq C(\mathcal{G}_1) = f_0 \leq \frac{2p + 2}{2p + 3}. \quad (26)$$

For p large the bound goes as

$$C_{\min} \leq 1 - \frac{1}{2p}. \quad (27)$$

This bound is independent of the graph connectivity and is consistent with the convergence of 2-regular graphs observed in [2].

Given a particular malicious MAXCUT instance with no small cycles, the convergence of QAOA will be inverse polynomial with a power of *at most* 1. Note that other graphs may converge much faster, as this bound only holds for graphs which have no cycles $\leq 2p + 1$. This means for a fixed cycle length, after some very large p convergence can be faster than this bound; the $p \rightarrow \infty$ behavior occurs only for the Bethe lattice, which has an infinite cycle length. The upper bound of Eq. (26) is plotted in Fig. 10. The computed values for 1, 2, and 3 do not come close to this limit, as this bound is loose. From

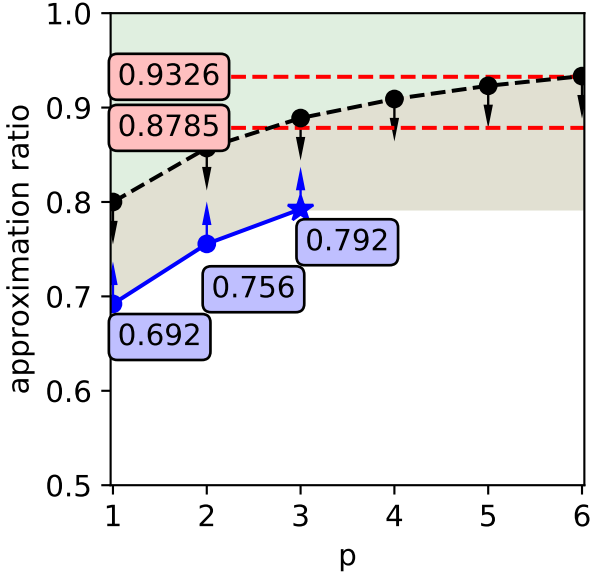


FIG. 10. Results of the paper: approximation ratios vs. p . Blue line is the worst case approximation ratio for $p = 1, 2, 3$; the $p = 3$ case (star) assumes the large loop conjecture. Red dashed are the Goemans-Williamson [19] and 3-regular [21] bounds. The minimum worst case approximation ratio is guaranteed to be below the black dashed line, which converges as $1 - 1/2p$.

Section VIII, the best classical algorithms for 3-regular MAXCUT have an approximation ratio of at least 0.9326; thus, p must be at least greater than 5 to have quantum advantage for a general 3-regular graph. This argument is based on a particular graph feature and the $p \leq 3$ guarantees tend below the bound, and so one might have a more pessimistic estimate on p due to special purpose classical algorithms and performance guarantees which may not saturate the bounds.

X. CONCLUSION

Bounding the performance of near-term quantum algorithms is critical to understand where, how, and why quantum computers may gain advantage in the NISQ era. In this paper, we find a worst case performance

guarantee for $p = 2$ QAOA solving MAXCUT on 3-regular graphs. This performance guarantee was found to be $C_2 \geq 0.7559$, which holds for any graph evaluated not just at its optimized angles, but for a fixed set of angles given by Table I. Because this set of angles is fixed, they can act as good initial guesses for a classical optimizer with a guaranteed approximation ratio.

More important than the number itself, the methods and the particular worst case graphs for which the bound was derived may be able to motivate particular ensembles of graph instances for which QAOA exhibits quantum advantage.

The worst case graphs for $p = 1$ and 2 were proved to be graphs with no cycles $\leq 2p + 1$. This was done via a graph reduction, replacing an edge with an expanded subgraph which distances the two original vertices of the edge and removes small cycles. The QAOA algorithm can only “see” the structure of a graph within some small number of steps, and so the effect of the graph reduction is twofold. In removing and lengthening cycles, due to its local nature the algorithm cannot distinguish between large even and odd length cycles. In expanding the edge into a larger subgraph, the two previously adjacent vertices of the edge are distanced so their previous relation is obscured to the algorithm.

These two properties stemming from the graph reduction suggest which graphs may have good QAOA solutions. Good graphs should have many small cycles, and should have a small-world structure [23] where only a logarithmic number of steps is necessary to move from one vertex to any other.

The properties presented here are heuristic and stem from the graph hierarchy, which is proved for $p \leq 2$ but can only be conjectured for $p > 2$. Future work remains to find more rigorous specifications and properties of graphs and problem instances on which it may be possible to demonstrate quantum advantage in QAOA.

Acknowledgements

This material is based upon work supported by the Defense Advanced Research Projects Agency (DARPA) under Contract No. HR001120C0068.

* Corresponding author: jonathan.wurtz@tufts.edu

¹ J. Preskill, *Quantum* **2**, 79 (2018).

² E. Farhi, J. Goldstone, and S. Gutmann, (2014), [arXiv:1411.4028](https://arxiv.org/abs/1411.4028) [quant-ph].

³ G. E. Crooks, (2018), [arXiv:1811.08419](https://arxiv.org/abs/1811.08419) [quant-ph].

⁴ M. B. Hastings, (2019), [arXiv:1905.07047](https://arxiv.org/abs/1905.07047) [quant-ph].

⁵ E. Farhi, J. Goldstone, and S. Gutmann, (2014), [arXiv:1412.6062v1](https://arxiv.org/abs/1412.6062v1) [quant-ph].

⁶ B. Barak, A. Moitra, R. O’Donnell, P. Raghavendra, O. Regev, D. Steurer, L. Trevisan, A. Vijayaraghavan,

D. Witmer, and J. Wright, (2015), [arXiv:1505.03424](https://arxiv.org/abs/1505.03424) [cs.CC].

⁷ E. Farhi, J. Goldstone, and S. Gutmann, (2015), [arXiv:1412.6062v2](https://arxiv.org/abs/1412.6062v2) [quant-ph].

⁸ M. Garey, D. Johnson, and L. Stockmeyer, *Theoretical Computer Science* **1**, 237 (1976).

⁹ E. Crosson, E. Farhi, C. Y.-Y. Lin, H.-H. Lin, and P. Shor, (2014), [arXiv:1401.7320](https://arxiv.org/abs/1401.7320) [quant-ph].

¹⁰ Z. Wang, S. Hadfield, Z. Jiang, and E. G. Rieffel, *Phys. Rev. A* **97**, 022304 (2018).

- ¹¹ M. Willsch, D. Willsch, F. Jin, H. De Raedt, and K. Michielsen, *Quantum Information Processing* **19**, 197 (2020).
- ¹² J. Larkin, M. Jonsson, D. Justice, and G. G. Guerreschi, (2020), [arXiv:2006.04831 \[quant-ph\]](#).
- ¹³ L. Zhou, S.-T. Wang, S. Choi, H. Pichler, and M. D. Lukin, *Phys. Rev. X* **10**, 021067 (2020).
- ¹⁴ Google AI Quantum and Collaborators, (2020), [arXiv:2004.04197 \[quant-ph\]](#).
- ¹⁵ K. Paton, *Commun. ACM* **12**, 514 (1969).
- ¹⁶ E. Farhi, D. Gamarnik, and S. Gutmann, (2020), [arXiv:2005.08747 \[quant-ph\]](#).
- ¹⁷ S. Sahni and T. Gonzalez, *J. ACM* **23**, 555–565 (1976).
- ¹⁸ J. Håstad, *J. ACM* **48**, 798–859 (2001).
- ¹⁹ M. X. Goemans and D. P. Williamson, *J. ACM* **42**, 1115–1145 (1995).
- ²⁰ M. Deza and M. Laurent, *Journal of Computational and Applied Mathematics* **55**, 217 (1994).
- ²¹ E. Halperin, D. Livnat, and U. Zwick, *Journal of Algorithms* **53**, 169 (2004).
- ²² E. Farhi and A. W. Harrow, (2016), [arXiv:1602.07674 \[quant-ph\]](#).
- ²³ D. J. Watts and S. H. Strogatz, *Nature* **393**, 440 (1998).

Appendix A: Computing optimal parameters γ, β

This Appendix details computing the optimal objective function f_λ for particular subgraphs. For each subgraph $\mathcal{S}_\lambda \in \{\mathcal{S}\}$, we wish to compute $\text{MAX} : f_\lambda(\gamma, \beta)$. First, generate the local objective function for the subgraph by including one clause $\frac{1}{2}(1 - \hat{\sigma}_z^i \hat{\sigma}_z^j)$ per edge $\langle ij \rangle$ in the subgraph, and similar for the local objective function on the special edge $\langle 0, 1 \rangle$ and mixing Hamiltonian \hat{B} of $\hat{\sigma}_x^i$ for each vertex i in the subgraph. We can compute expectation values exactly, which similarly enables access to derivatives of the objective function

$$\begin{aligned} \partial_{\gamma_1} \langle \hat{C} \rangle &= [\partial_{\gamma_1} \langle \gamma, \beta |] \hat{C} | \gamma, \beta \rangle + \langle \gamma, \beta | \hat{C} [\partial_{\gamma_1} | \gamma, \beta \rangle] \quad (\text{A1}) \\ \partial_{\gamma_1} | \gamma, \beta \rangle &= -i e^{-i\beta_p \hat{B}} e^{-i\gamma_p \hat{C}} (\dots) e^{-i\beta_1 \hat{B}} (\hat{C} e^{i\gamma_1 \hat{C}}) | \gamma, \beta \rangle \end{aligned}$$

and similar for the other γ, β , with ellipsis denoting the other $2p - 4$ generators. With access to both the exact expectation values and derivatives, parameters were optimized via a multistart gradient ascent algorithm. For each subgraph, initial parameters were chosen uniformly in parameter space, which is compact in $\{[-\pi/4, \pi/4], [-\pi, \pi]\}^p$. Note that unlike for general QAOA, β is periodic modulo $\pi/2$, due to \mathbb{Z}_2 symmetry, eg $\hat{\sigma}_z \rightarrow -\hat{\sigma}_z$. This is because the unitary over the mixing term

$$e^{i(\beta+\pi/2)\hat{B}} = \left(\prod_i e^{i\pi/2\hat{\sigma}_x^i} \right) e^{i\beta\hat{B}} = \hat{\mathbb{Z}}_2 e^{i\beta\hat{B}}, \quad (\text{A2})$$

and $[\hat{\mathbb{Z}}_2, \hat{B}] = [\hat{\mathbb{Z}}_2, \hat{C}] = 0$. For each optimization, 25 random initial parameters were chosen to find a maxima with high probability. To find all degenerate maxima of a subgraph, initial parameters were chosen on a mesh, and each also optimized with gradient descent. At each step, the parameters are updated to change along the direction with the largest gradient, with size $0.075|\vec{\nabla} \langle C \rangle|$, where the constant is an implicit choice of the maximum second derivative. A particular optimization ends when the expectation value changes by less than 10^{-5} .

For the $p = 3$ tree, a free optimization was used to speed up the calculation by reducing the Hilbert space using symmetry. Every graph has a certain set of isomorphisms, eg relabeling of each vertex. These isomorphisms define swap operators which commute with the generators \hat{B} and \hat{C} , and thus the eigenvalues are good quantum numbers defining conserved subspaces of the Hilbert space. The initial wavefunction $|+\rangle$ is unchanged under any relabeling of indices, and so lives in the $+1$ subspace of all isomorphisms. While this reduction is in principle possible for any subgraph, it is particularly simple for the recognizable swap symmetries of the tree. Swapping any two “branches” of the tree leaves the wavefunction

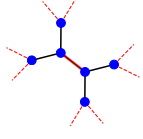
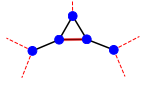
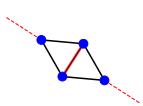
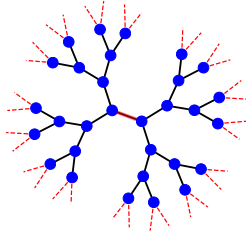
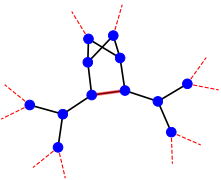
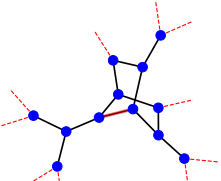
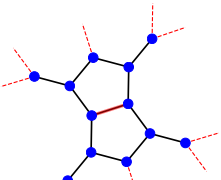
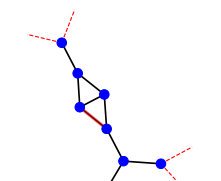
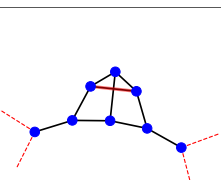
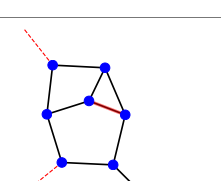
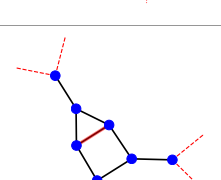
	Index	1, 0
	c_{\max}	5/5
	f_0	0.6924
	Envs.	1
	γ_1	35°
	β_1	22°
	Index	1, 1
	c_{\max}	4/5
	f_1	0.6369
	Envs.	2
	f'_1	0.6467
	γ_1	-211°
	β_1	108°
	Index	1, 2
	c_{\max}	4/5
	f_2	0.5813
	Envs.	1
	f'_2	0.6163
	γ_1	-28°
	β_1	164°
	Index	3, 0
	c_{\max}	29/29
	f_0	0.7924
	Envs.	1
	γ_1	156°
	β_1	-35°
	γ_2	-46°
	β_2	-27°
	γ_3	-54°
	β_3	-14°

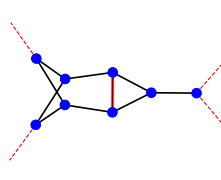
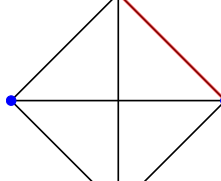
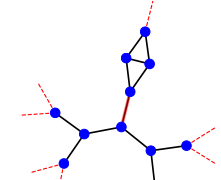
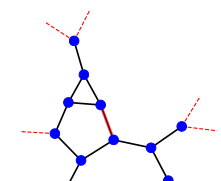
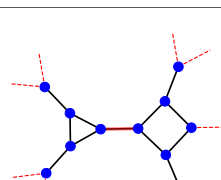
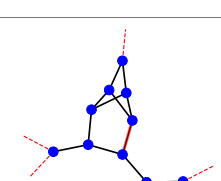
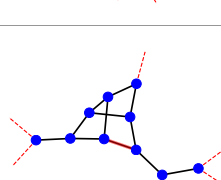
TABLE II. Numerical data for $p = 1, 2$ and a specific $p = 3$ graph. Row 1 enumerates subgraphs. Row 2 counts the local **MAXCUT** value, cutting N of M total edges. Row 3 is the expectation value for the edge evaluated at the angles of table I. Row 4 is the number of relevant graph environments which the subgraph can be in. Row 5 is the maximum expectation value of the subgraph, optimized at the angles of rows 6+. Image is the representation of the subgraph; red dashed represent edges connecting to the rest of the graph, while red solid represents the special center edge.

invariant, and so only symmetric combinations remain. For two vertices (eg $p = 0$), this is only three states: both up, both down, and the triplet state. For 6 vertices, there are 3 isomorphisms: swapping the left or right two vertices, or reflecting the three left with three right. Under these symmetries there are 21 states. This can be done recursively by knowing that given two indistinguishable Hilbert spaces of dimension \mathcal{D} , there are only $\mathcal{D}(\mathcal{D}+1)/2$ symmetric combinations. Using this, for $p = 2$ there are 903 states; for $p = 3$ there are $1,631,721 \approx 2^{20.6}$; and for $p = 4$ there are $5,325,028,475,403 \approx 2^{42.3}$. There is an additional factor of ≈ 2 , as the generators have a \mathbb{Z}_2 spin flip symmetry $\hat{\sigma}_z \leftrightarrow -\hat{\sigma}_z$. In principle, it may be possible to simulate the worst case 4-tree exactly, as 41 qubits is within range of classical simulatability, but is beyond the scope of this work.

	Index	2, 0
	c_{\max}	13/13
	f_0	0.7559
	Envs.	1
	f'_0	0.7559
	γ_1	28°
	β_1	58°
	β_2	73°
	Index	2, 1
	c_{\max}	9/10
	f_1	0.6456
	Envs.	141
	f'_1	0.6620
	γ_1	-35°
	β_1	-75°
	β_2	-99°
	Index	2, 2
	c_{\max}	6/7
	f_2	0.4541
	Envs.	18
	f'_2	0.7000
	γ_1	36°
	β_1	46°
	β_2	33°
	Index	2, 3
	c_{\max}	13/13
	f_3	0.7448
	Envs.	1
	f'_3	0.7462
	γ_1	154°
	β_1	60°
	β_2	16°
	Index	2, 4
	c_{\max}	12/13
	f_4	0.7502
	Envs.	137
	f'_4	0.7509
	γ_1	208°
	β_1	30°
	β_2	105°
	Index	2, 5
	c_{\max}	9/10
	f_5	0.6300
	Envs.	38
	f'_5	0.6564
	γ_1	35°
	β_1	-13°
	β_2	9°
	Index	2, 6
	c_{\max}	9/10
	f_6	0.6358
	Envs.	148
	f'_6	0.6605
	γ_1	-144°
	β_1	-76°
	β_2	-81°

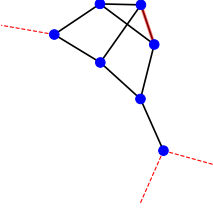
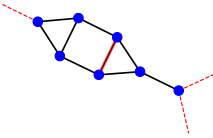
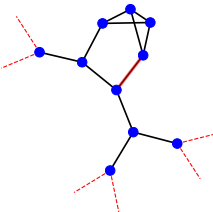
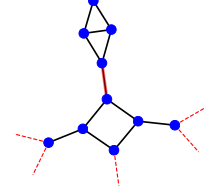
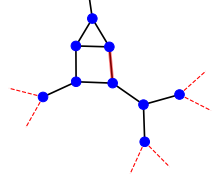
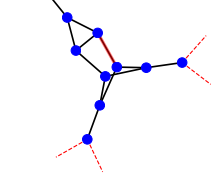
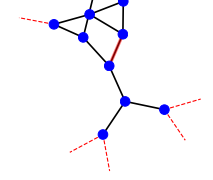
	Index	2, 7
	c_{\max}	6/7
	f_7	0.4258
	Envs.	1
	f'_7	0.7492
	γ_1	217°
	β_1	42°
	β_2	-28°
	Index	2, 8
	c_{\max}	11/12
	f_8	0.7919
	Envs.	1
	f'_8	0.8038
	γ_1	-33°
	β_1	-62°
	β_2	-106°
	Index	2, 9
	c_{\max}	12/13
	f_9	0.7334
	Envs.	12
	f'_9	0.7386
	γ_1	-155°
	β_1	29°
	β_2	-133°
	Index	2, 10
	c_{\max}	13/13
	f_{10}	0.7339
	Envs.	1
	f'_{10}	0.7399
	γ_1	49°
	β_1	18°
	β_2	40°
	Index	2, 11
	c_{\max}	12/13
	f_{11}	0.7396
	Envs.	112
	f'_{11}	0.7422
	γ_1	-26°
	β_1	30°
	β_2	75°
	Index	2, 12
	c_{\max}	13/13
	f_{12}	0.7334
	Envs.	1
	f'_{12}	0.7409
	γ_1	230°
	β_1	72°
	β_2	-50°
	Index	2, 13
	c_{\max}	12/12
	f_{13}	0.7902
	Envs.	1073
	f'_{13}	0.7959
	γ_1	151°
	β_1	-34°
	β_2	20°

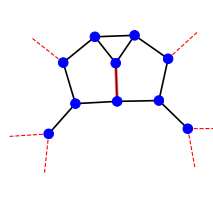
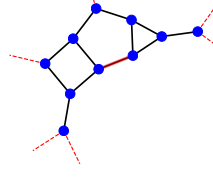
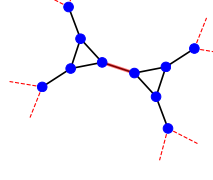
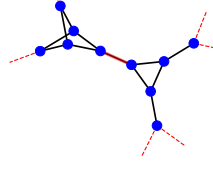
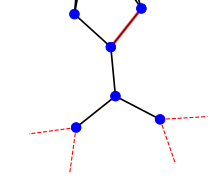
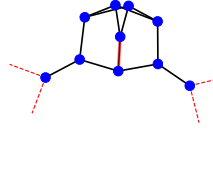
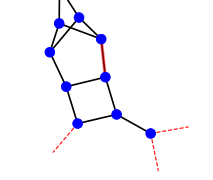
	<table> <tr><td>Index</td><td>2, 14</td></tr> <tr><td>c_{\max}</td><td>12/13</td></tr> <tr><td>f_{14}</td><td>0.7445</td></tr> <tr><td>Envs.</td><td>11</td></tr> <tr><td>f'_{14}</td><td>0.7468</td></tr> <tr><td>γ_1</td><td>-152°</td></tr> <tr><td>β_1</td><td>-60°</td></tr> <tr><td>γ_2</td><td>51°</td></tr> <tr><td>β_2</td><td>15°</td></tr> </table>	Index	2, 14	c_{\max}	12/13	f_{14}	0.7445	Envs.	11	f'_{14}	0.7468	γ_1	-152°	β_1	-60°	γ_2	51°	β_2	15°
Index	2, 14																		
c_{\max}	12/13																		
f_{14}	0.7445																		
Envs.	11																		
f'_{14}	0.7468																		
γ_1	-152°																		
β_1	-60°																		
γ_2	51°																		
β_2	15°																		
	<table> <tr><td>Index</td><td>2, 15</td></tr> <tr><td>c_{\max}</td><td>12/13</td></tr> <tr><td>f_{15}</td><td>0.7445</td></tr> <tr><td>Envs.</td><td>135</td></tr> <tr><td>f'_{15}</td><td>0.7469</td></tr> <tr><td>γ_1</td><td>152°</td></tr> <tr><td>β_1</td><td>60°</td></tr> <tr><td>γ_2</td><td>-51°</td></tr> <tr><td>β_2</td><td>75°</td></tr> </table>	Index	2, 15	c_{\max}	12/13	f_{15}	0.7445	Envs.	135	f'_{15}	0.7469	γ_1	152°	β_1	60°	γ_2	-51°	β_2	75°
Index	2, 15																		
c_{\max}	12/13																		
f_{15}	0.7445																		
Envs.	135																		
f'_{15}	0.7469																		
γ_1	152°																		
β_1	60°																		
γ_2	-51°																		
β_2	75°																		
	<table> <tr><td>Index</td><td>2, 16</td></tr> <tr><td>c_{\max}</td><td>12/13</td></tr> <tr><td>f_{16}</td><td>0.7442</td></tr> <tr><td>Envs.</td><td>791</td></tr> <tr><td>f'_{16}</td><td>0.7466</td></tr> <tr><td>γ_1</td><td>207°</td></tr> <tr><td>β_1</td><td>-61°</td></tr> <tr><td>γ_2</td><td>50°</td></tr> <tr><td>β_2</td><td>15°</td></tr> </table>	Index	2, 16	c_{\max}	12/13	f_{16}	0.7442	Envs.	791	f'_{16}	0.7466	γ_1	207°	β_1	-61°	γ_2	50°	β_2	15°
Index	2, 16																		
c_{\max}	12/13																		
f_{16}	0.7442																		
Envs.	791																		
f'_{16}	0.7466																		
γ_1	207°																		
β_1	-61°																		
γ_2	50°																		
β_2	15°																		
	<table> <tr><td>Index</td><td>2, 17</td></tr> <tr><td>c_{\max}</td><td>8/9</td></tr> <tr><td>f_{17}</td><td>0.7125</td></tr> <tr><td>Envs.</td><td>25</td></tr> <tr><td>f'_{17}</td><td>0.7273</td></tr> <tr><td>γ_1</td><td>-213°</td></tr> <tr><td>β_1</td><td>67°</td></tr> <tr><td>γ_2</td><td>116°</td></tr> <tr><td>β_2</td><td>16°</td></tr> </table>	Index	2, 17	c_{\max}	8/9	f_{17}	0.7125	Envs.	25	f'_{17}	0.7273	γ_1	-213°	β_1	67°	γ_2	116°	β_2	16°
Index	2, 17																		
c_{\max}	8/9																		
f_{17}	0.7125																		
Envs.	25																		
f'_{17}	0.7273																		
γ_1	-213°																		
β_1	67°																		
γ_2	116°																		
β_2	16°																		
	<table> <tr><td>Index</td><td>2, 18</td></tr> <tr><td>c_{\max}</td><td>9/10</td></tr> <tr><td>f_{18}</td><td>0.6047</td></tr> <tr><td>Envs.</td><td>2</td></tr> <tr><td>f'_{18}</td><td>0.6614</td></tr> <tr><td>γ_1</td><td>-39°</td></tr> <tr><td>β_1</td><td>-55°</td></tr> <tr><td>γ_2</td><td>-109°</td></tr> <tr><td>β_2</td><td>70°</td></tr> </table>	Index	2, 18	c_{\max}	9/10	f_{18}	0.6047	Envs.	2	f'_{18}	0.6614	γ_1	-39°	β_1	-55°	γ_2	-109°	β_2	70°
Index	2, 18																		
c_{\max}	9/10																		
f_{18}	0.6047																		
Envs.	2																		
f'_{18}	0.6614																		
γ_1	-39°																		
β_1	-55°																		
γ_2	-109°																		
β_2	70°																		
	<table> <tr><td>Index</td><td>2, 19</td></tr> <tr><td>c_{\max}</td><td>9/10</td></tr> <tr><td>f_{19}</td><td>0.6207</td></tr> <tr><td>Envs.</td><td>18</td></tr> <tr><td>f'_{19}</td><td>0.6554</td></tr> <tr><td>γ_1</td><td>-33°</td></tr> <tr><td>β_1</td><td>11°</td></tr> <tr><td>γ_2</td><td>75°</td></tr> <tr><td>β_2</td><td>80°</td></tr> </table>	Index	2, 19	c_{\max}	9/10	f_{19}	0.6207	Envs.	18	f'_{19}	0.6554	γ_1	-33°	β_1	11°	γ_2	75°	β_2	80°
Index	2, 19																		
c_{\max}	9/10																		
f_{19}	0.6207																		
Envs.	18																		
f'_{19}	0.6554																		
γ_1	-33°																		
β_1	11°																		
γ_2	75°																		
β_2	80°																		
	<table> <tr><td>Index</td><td>2, 20</td></tr> <tr><td>c_{\max}</td><td>8/9</td></tr> <tr><td>f_{20}</td><td>0.6998</td></tr> <tr><td>Envs.</td><td>157</td></tr> <tr><td>f'_{20}</td><td>0.7209</td></tr> <tr><td>γ_1</td><td>219°</td></tr> <tr><td>β_1</td><td>-59°</td></tr> <tr><td>γ_2</td><td>-126°</td></tr> <tr><td>β_2</td><td>-25°</td></tr> </table>	Index	2, 20	c_{\max}	8/9	f_{20}	0.6998	Envs.	157	f'_{20}	0.7209	γ_1	219°	β_1	-59°	γ_2	-126°	β_2	-25°
Index	2, 20																		
c_{\max}	8/9																		
f_{20}	0.6998																		
Envs.	157																		
f'_{20}	0.7209																		
γ_1	219°																		
β_1	-59°																		
γ_2	-126°																		
β_2	-25°																		

	<table> <tr><td>Index</td><td>2, 21</td></tr> <tr><td>c_{\max}</td><td>9/10</td></tr> <tr><td>f_{21}</td><td>0.6257</td></tr> <tr><td>Envs.</td><td>23</td></tr> <tr><td>f'_{21}</td><td>0.6590</td></tr> <tr><td>γ_1</td><td>147°</td></tr> <tr><td>β_1</td><td>-14°</td></tr> <tr><td>γ_2</td><td>80°</td></tr> <tr><td>β_2</td><td>8°</td></tr> </table>	Index	2, 21	c_{\max}	9/10	f_{21}	0.6257	Envs.	23	f'_{21}	0.6590	γ_1	147°	β_1	-14°	γ_2	80°	β_2	8°
Index	2, 21																		
c_{\max}	9/10																		
f_{21}	0.6257																		
Envs.	23																		
f'_{21}	0.6590																		
γ_1	147°																		
β_1	-14°																		
γ_2	80°																		
β_2	8°																		
	<table> <tr><td>Index</td><td>2, 22</td></tr> <tr><td>c_{\max}</td><td>4/6</td></tr> <tr><td>f_{22}</td><td>0.5739</td></tr> <tr><td>Envs.</td><td>1</td></tr> <tr><td>f'_{22}</td><td>0.6666</td></tr> <tr><td>γ_1</td><td>115°</td></tr> <tr><td>β_1</td><td>51°</td></tr> <tr><td>γ_2</td><td>79°</td></tr> <tr><td>β_2</td><td>-24°</td></tr> </table>	Index	2, 22	c_{\max}	4/6	f_{22}	0.5739	Envs.	1	f'_{22}	0.6666	γ_1	115°	β_1	51°	γ_2	79°	β_2	-24°
Index	2, 22																		
c_{\max}	4/6																		
f_{22}	0.5739																		
Envs.	1																		
f'_{22}	0.6666																		
γ_1	115°																		
β_1	51°																		
γ_2	79°																		
β_2	-24°																		
	<table> <tr><td>Index</td><td>2, 23</td></tr> <tr><td>c_{\max}</td><td>11/12</td></tr> <tr><td>f_{23}</td><td>0.7777</td></tr> <tr><td>Envs.</td><td>1</td></tr> <tr><td>f'_{23}</td><td>0.7840</td></tr> <tr><td>γ_1</td><td>30°</td></tr> <tr><td>β_1</td><td>-28°</td></tr> <tr><td>γ_2</td><td>54°</td></tr> <tr><td>β_2</td><td>-106°</td></tr> </table>	Index	2, 23	c_{\max}	11/12	f_{23}	0.7777	Envs.	1	f'_{23}	0.7840	γ_1	30°	β_1	-28°	γ_2	54°	β_2	-106°
Index	2, 23																		
c_{\max}	11/12																		
f_{23}	0.7777																		
Envs.	1																		
f'_{23}	0.7840																		
γ_1	30°																		
β_1	-28°																		
γ_2	54°																		
β_2	-106°																		
	<table> <tr><td>Index</td><td>2, 24</td></tr> <tr><td>c_{\max}</td><td>11/12</td></tr> <tr><td>f_{24}</td><td>0.7851</td></tr> <tr><td>Envs.</td><td>45</td></tr> <tr><td>f'_{24}</td><td>0.7996</td></tr> <tr><td>γ_1</td><td>-33°</td></tr> <tr><td>β_1</td><td>-63°</td></tr> <tr><td>γ_2</td><td>-60°</td></tr> <tr><td>β_2</td><td>-74°</td></tr> </table>	Index	2, 24	c_{\max}	11/12	f_{24}	0.7851	Envs.	45	f'_{24}	0.7996	γ_1	-33°	β_1	-63°	γ_2	-60°	β_2	-74°
Index	2, 24																		
c_{\max}	11/12																		
f_{24}	0.7851																		
Envs.	45																		
f'_{24}	0.7996																		
γ_1	-33°																		
β_1	-63°																		
γ_2	-60°																		
β_2	-74°																		
	<table> <tr><td>Index</td><td>2, 25</td></tr> <tr><td>c_{\max}</td><td>11/12</td></tr> <tr><td>f_{25}</td><td>0.7823</td></tr> <tr><td>Envs.</td><td>1</td></tr> <tr><td>f'_{25}</td><td>0.7904</td></tr> <tr><td>γ_1</td><td>-148°</td></tr> <tr><td>β_1</td><td>-62°</td></tr> <tr><td>γ_2</td><td>57°</td></tr> <tr><td>β_2</td><td>-74°</td></tr> </table>	Index	2, 25	c_{\max}	11/12	f_{25}	0.7823	Envs.	1	f'_{25}	0.7904	γ_1	-148°	β_1	-62°	γ_2	57°	β_2	-74°
Index	2, 25																		
c_{\max}	11/12																		
f_{25}	0.7823																		
Envs.	1																		
f'_{25}	0.7904																		
γ_1	-148°																		
β_1	-62°																		
γ_2	57°																		
β_2	-74°																		
	<table> <tr><td>Index</td><td>2, 26</td></tr> <tr><td>c_{\max}</td><td>12/13</td></tr> <tr><td>f_{26}</td><td>0.7235</td></tr> <tr><td>Envs.</td><td>5</td></tr> <tr><td>f'_{26}</td><td>0.7341</td></tr> <tr><td>γ_1</td><td>129°</td></tr> <tr><td>β_1</td><td>16°</td></tr> <tr><td>γ_2</td><td>20°</td></tr> <tr><td>β_2</td><td>52°</td></tr> </table>	Index	2, 26	c_{\max}	12/13	f_{26}	0.7235	Envs.	5	f'_{26}	0.7341	γ_1	129°	β_1	16°	γ_2	20°	β_2	52°
Index	2, 26																		
c_{\max}	12/13																		
f_{26}	0.7235																		
Envs.	5																		
f'_{26}	0.7341																		
γ_1	129°																		
β_1	16°																		
γ_2	20°																		
β_2	52°																		
	<table> <tr><td>Index</td><td>2, 27</td></tr> <tr><td>c_{\max}</td><td>12/13</td></tr> <tr><td>f_{27}</td><td>0.7282</td></tr> <tr><td>Envs.</td><td>3</td></tr> <tr><td>f'_{27}</td><td>0.7360</td></tr> <tr><td>γ_1</td><td>154°</td></tr> <tr><td>β_1</td><td>-28°</td></tr> <tr><td>γ_2</td><td>133°</td></tr> <tr><td>β_2</td><td>13°</td></tr> </table>	Index	2, 27	c_{\max}	12/13	f_{27}	0.7282	Envs.	3	f'_{27}	0.7360	γ_1	154°	β_1	-28°	γ_2	133°	β_2	13°
Index	2, 27																		
c_{\max}	12/13																		
f_{27}	0.7282																		
Envs.	3																		
f'_{27}	0.7360																		
γ_1	154°																		
β_1	-28°																		
γ_2	133°																		
β_2	13°																		

	Index	2, 28
	c_{\max}	12/13
	f_{28}	0.7279
	Envs.	35
	f'_{28}	0.7358
	γ_1	26°
	β_1	-28°
	β_2	-103°
	Index	2, 29
	c_{\max}	12/13
	f_{29}	0.7230
	Envs.	6
	f'_{29}	0.7351
	γ_1	-129°
	β_1	-17°
	β_2	52°
	Index	2, 30
	c_{\max}	13/13
	f_{30}	0.7222
	Envs.	1
	f'_{30}	0.7425
	γ_1	39°
	β_1	51°
	β_2	-20°
	Index	2, 31
	c_{\max}	12/12
	f_{31}	0.7778
	Envs.	172
	f'_{31}	0.7833
	γ_1	27°
	β_1	57°
	β_2	-19°
	Index	2, 32
	c_{\max}	12/13
	f_{32}	0.7344
	Envs.	29
	f'_{32}	0.7390
	γ_1	-26°
	β_1	-61°
	β_2	104°
	Index	2, 33
	c_{\max}	12/13
	f_{33}	0.7340
	Envs.	231
	f'_{33}	0.7388
	γ_1	154°
	β_1	61°
	β_2	-76°
	Index	2, 34
	c_{\max}	12/13
	f_{34}	0.7286
	Envs.	31
	f'_{34}	0.7378
	γ_1	-130°
	β_1	72°
	β_2	-40°

	Index	2, 35
	c_{\max}	11/12
	f_{35}	0.7831
	Envs.	30
	f'_{35}	0.7852
	γ_1	152°
	β_1	-33°
	β_2	18°
	Index	2, 36
	c_{\max}	11/12
	f_{36}	0.7840
	Envs.	319
	f'_{36}	0.7866
	γ_1	152°
	β_1	57°
	β_2	-19°
	Index	2, 37
	c_{\max}	11/12
	f_{37}	0.7859
	Envs.	1161
	f'_{37}	0.7890
	γ_1	-29°
	β_1	33°
	β_2	19°
	Index	2, 38
	c_{\max}	12/13
	f_{38}	0.7381
	Envs.	115
	f'_{38}	0.7431
	γ_1	28°
	β_1	61°
	β_2	-130°
	Index	2, 39
	c_{\max}	12/13
	f_{39}	0.7385
	Envs.	163
	f'_{39}	0.7433
	γ_1	28°
	β_1	61°
	β_2	-76°
	Index	2, 40
	c_{\max}	7/9
	f_{40}	0.7017
	Envs.	6
	f'_{40}	0.7206
	γ_1	-32°
	β_1	-68°
	β_2	-75°
	Index	2, 41
	c_{\max}	9/10
	f_{41}	0.5954
	Envs.	1
	f'_{41}	0.6528
	γ_1	-51°
	β_1	-7°
	β_2	-64°

	<table> <tr><td>Index</td><td>2, 42</td></tr> <tr><td>c_{\max}</td><td>8/9</td></tr> <tr><td>f_{42}</td><td>0.6823</td></tr> <tr><td>Envs.</td><td>9</td></tr> <tr><td>f'_{42}</td><td>0.6885</td></tr> <tr><td>γ_1</td><td>35°</td></tr> <tr><td>β_1</td><td>-28°</td></tr> <tr><td>γ_2</td><td>-126°</td></tr> <tr><td>β_2</td><td>21°</td></tr> </table>	Index	2, 42	c_{\max}	8/9	f_{42}	0.6823	Envs.	9	f'_{42}	0.6885	γ_1	35°	β_1	-28°	γ_2	-126°	β_2	21°
Index	2, 42																		
c_{\max}	8/9																		
f_{42}	0.6823																		
Envs.	9																		
f'_{42}	0.6885																		
γ_1	35°																		
β_1	-28°																		
γ_2	-126°																		
β_2	21°																		
	<table> <tr><td>Index</td><td>2, 43</td></tr> <tr><td>c_{\max}</td><td>7/9</td></tr> <tr><td>f_{43}</td><td>0.6876</td></tr> <tr><td>Envs.</td><td>6</td></tr> <tr><td>f'_{43}</td><td>0.6914</td></tr> <tr><td>γ_1</td><td>-148°</td></tr> <tr><td>β_1</td><td>-62°</td></tr> <tr><td>γ_2</td><td>54°</td></tr> <tr><td>β_2</td><td>18°</td></tr> </table>	Index	2, 43	c_{\max}	7/9	f_{43}	0.6876	Envs.	6	f'_{43}	0.6914	γ_1	-148°	β_1	-62°	γ_2	54°	β_2	18°
Index	2, 43																		
c_{\max}	7/9																		
f_{43}	0.6876																		
Envs.	6																		
f'_{43}	0.6914																		
γ_1	-148°																		
β_1	-62°																		
γ_2	54°																		
β_2	18°																		
	<table> <tr><td>Index</td><td>2, 44</td></tr> <tr><td>c_{\max}</td><td>10/12</td></tr> <tr><td>f_{44}</td><td>0.7641</td></tr> <tr><td>Envs.</td><td>3</td></tr> <tr><td>f'_{44}</td><td>0.7764</td></tr> <tr><td>γ_1</td><td>150°</td></tr> <tr><td>β_1</td><td>-27°</td></tr> <tr><td>γ_2</td><td>-54°</td></tr> <tr><td>β_2</td><td>75°</td></tr> </table>	Index	2, 44	c_{\max}	10/12	f_{44}	0.7641	Envs.	3	f'_{44}	0.7764	γ_1	150°	β_1	-27°	γ_2	-54°	β_2	75°
Index	2, 44																		
c_{\max}	10/12																		
f_{44}	0.7641																		
Envs.	3																		
f'_{44}	0.7764																		
γ_1	150°																		
β_1	-27°																		
γ_2	-54°																		
β_2	75°																		
	<table> <tr><td>Index</td><td>2, 45</td></tr> <tr><td>c_{\max}</td><td>11/12</td></tr> <tr><td>f_{45}</td><td>0.7677</td></tr> <tr><td>Envs.</td><td>1</td></tr> <tr><td>f'_{45}</td><td>0.7739</td></tr> <tr><td>γ_1</td><td>152°</td></tr> <tr><td>β_1</td><td>62°</td></tr> <tr><td>γ_2</td><td>-52°</td></tr> <tr><td>β_2</td><td>-105°</td></tr> </table>	Index	2, 45	c_{\max}	11/12	f_{45}	0.7677	Envs.	1	f'_{45}	0.7739	γ_1	152°	β_1	62°	γ_2	-52°	β_2	-105°
Index	2, 45																		
c_{\max}	11/12																		
f_{45}	0.7677																		
Envs.	1																		
f'_{45}	0.7739																		
γ_1	152°																		
β_1	62°																		
γ_2	-52°																		
β_2	-105°																		
	<table> <tr><td>Index</td><td>2, 46</td></tr> <tr><td>c_{\max}</td><td>10/11</td></tr> <tr><td>f_{46}</td><td>0.8260</td></tr> <tr><td>Envs.</td><td>58</td></tr> <tr><td>f'_{46}</td><td>0.8348</td></tr> <tr><td>γ_1</td><td>-148°</td></tr> <tr><td>β_1</td><td>-59°</td></tr> <tr><td>γ_2</td><td>55°</td></tr> <tr><td>β_2</td><td>-71°</td></tr> </table>	Index	2, 46	c_{\max}	10/11	f_{46}	0.8260	Envs.	58	f'_{46}	0.8348	γ_1	-148°	β_1	-59°	γ_2	55°	β_2	-71°
Index	2, 46																		
c_{\max}	10/11																		
f_{46}	0.8260																		
Envs.	58																		
f'_{46}	0.8348																		
γ_1	-148°																		
β_1	-59°																		
γ_2	55°																		
β_2	-71°																		
	<table> <tr><td>Index</td><td>2, 47</td></tr> <tr><td>c_{\max}</td><td>11/12</td></tr> <tr><td>f_{47}</td><td>0.7687</td></tr> <tr><td>Envs.</td><td>2</td></tr> <tr><td>f'_{47}</td><td>0.7827</td></tr> <tr><td>γ_1</td><td>-32°</td></tr> <tr><td>β_1</td><td>27°</td></tr> <tr><td>γ_2</td><td>-57°</td></tr> <tr><td>β_2</td><td>15°</td></tr> </table>	Index	2, 47	c_{\max}	11/12	f_{47}	0.7687	Envs.	2	f'_{47}	0.7827	γ_1	-32°	β_1	27°	γ_2	-57°	β_2	15°
Index	2, 47																		
c_{\max}	11/12																		
f_{47}	0.7687																		
Envs.	2																		
f'_{47}	0.7827																		
γ_1	-32°																		
β_1	27°																		
γ_2	-57°																		
β_2	15°																		
	<table> <tr><td>Index</td><td>2, 48</td></tr> <tr><td>c_{\max}</td><td>10/12</td></tr> <tr><td>f_{48}</td><td>0.7784</td></tr> <tr><td>Envs.</td><td>9</td></tr> <tr><td>f'_{48}</td><td>0.7964</td></tr> <tr><td>γ_1</td><td>146°</td></tr> <tr><td>β_1</td><td>-27°</td></tr> <tr><td>γ_2</td><td>119°</td></tr> <tr><td>β_2</td><td>15°</td></tr> </table>	Index	2, 48	c_{\max}	10/12	f_{48}	0.7784	Envs.	9	f'_{48}	0.7964	γ_1	146°	β_1	-27°	γ_2	119°	β_2	15°
Index	2, 48																		
c_{\max}	10/12																		
f_{48}	0.7784																		
Envs.	9																		
f'_{48}	0.7964																		
γ_1	146°																		
β_1	-27°																		
γ_2	119°																		
β_2	15°																		

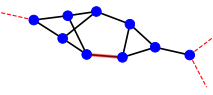
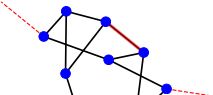
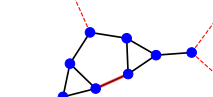
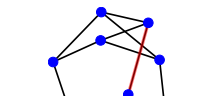
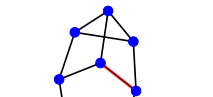
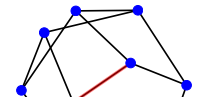
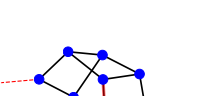
	<table> <tr><td>Index</td><td>2, 49</td></tr> <tr><td>c_{\max}</td><td>10/12</td></tr> <tr><td>f_{49}</td><td>0.7779</td></tr> <tr><td>Envs.</td><td>56</td></tr> <tr><td>f'_{49}</td><td>0.7954</td></tr> <tr><td>γ_1</td><td>146°</td></tr> <tr><td>β_1</td><td>-27°</td></tr> <tr><td>γ_2</td><td>-61°</td></tr> <tr><td>β_2</td><td>-15°</td></tr> </table>	Index	2, 49	c_{\max}	10/12	f_{49}	0.7779	Envs.	56	f'_{49}	0.7954	γ_1	146°	β_1	-27°	γ_2	-61°	β_2	-15°
Index	2, 49																		
c_{\max}	10/12																		
f_{49}	0.7779																		
Envs.	56																		
f'_{49}	0.7954																		
γ_1	146°																		
β_1	-27°																		
γ_2	-61°																		
β_2	-15°																		
	<table> <tr><td>Index</td><td>2, 50</td></tr> <tr><td>c_{\max}</td><td>11/12</td></tr> <tr><td>f_{50}</td><td>0.7760</td></tr> <tr><td>Envs.</td><td>21</td></tr> <tr><td>f'_{50}</td><td>0.7868</td></tr> <tr><td>γ_1</td><td>32°</td></tr> <tr><td>β_1</td><td>63°</td></tr> <tr><td>γ_2</td><td>-123°</td></tr> <tr><td>β_2</td><td>16°</td></tr> </table>	Index	2, 50	c_{\max}	11/12	f_{50}	0.7760	Envs.	21	f'_{50}	0.7868	γ_1	32°	β_1	63°	γ_2	-123°	β_2	16°
Index	2, 50																		
c_{\max}	11/12																		
f_{50}	0.7760																		
Envs.	21																		
f'_{50}	0.7868																		
γ_1	32°																		
β_1	63°																		
γ_2	-123°																		
β_2	16°																		
	<table> <tr><td>Index</td><td>2, 51</td></tr> <tr><td>c_{\max}</td><td>9/11</td></tr> <tr><td>f_{51}</td><td>0.8228</td></tr> <tr><td>Envs.</td><td>1</td></tr> <tr><td>f'_{51}</td><td>0.8624</td></tr> <tr><td>γ_1</td><td>-35°</td></tr> <tr><td>β_1</td><td>-65°</td></tr> <tr><td>γ_2</td><td>113°</td></tr> <tr><td>β_2</td><td>-17°</td></tr> </table>	Index	2, 51	c_{\max}	9/11	f_{51}	0.8228	Envs.	1	f'_{51}	0.8624	γ_1	-35°	β_1	-65°	γ_2	113°	β_2	-17°
Index	2, 51																		
c_{\max}	9/11																		
f_{51}	0.8228																		
Envs.	1																		
f'_{51}	0.8624																		
γ_1	-35°																		
β_1	-65°																		
γ_2	113°																		
β_2	-17°																		
	<table> <tr><td>Index</td><td>2, 52</td></tr> <tr><td>c_{\max}</td><td>11/12</td></tr> <tr><td>f_{52}</td><td>0.7729</td></tr> <tr><td>Envs.</td><td>1</td></tr> <tr><td>f'_{52}</td><td>0.7795</td></tr> <tr><td>γ_1</td><td>150°</td></tr> <tr><td>β_1</td><td>62°</td></tr> <tr><td>γ_2</td><td>-53°</td></tr> <tr><td>β_2</td><td>74°</td></tr> </table>	Index	2, 52	c_{\max}	11/12	f_{52}	0.7729	Envs.	1	f'_{52}	0.7795	γ_1	150°	β_1	62°	γ_2	-53°	β_2	74°
Index	2, 52																		
c_{\max}	11/12																		
f_{52}	0.7729																		
Envs.	1																		
f'_{52}	0.7795																		
γ_1	150°																		
β_1	62°																		
γ_2	-53°																		
β_2	74°																		
	<table> <tr><td>Index</td><td>2, 53</td></tr> <tr><td>c_{\max}</td><td>12/13</td></tr> <tr><td>f_{53}</td><td>0.7131</td></tr> <tr><td>Envs.</td><td>1</td></tr> <tr><td>f'_{53}</td><td>0.7299</td></tr> <tr><td>γ_1</td><td>48°</td></tr> <tr><td>β_1</td><td>-73°</td></tr> <tr><td>γ_2</td><td>-18°</td></tr> <tr><td>β_2</td><td>-39°</td></tr> </table>	Index	2, 53	c_{\max}	12/13	f_{53}	0.7131	Envs.	1	f'_{53}	0.7299	γ_1	48°	β_1	-73°	γ_2	-18°	β_2	-39°
Index	2, 53																		
c_{\max}	12/13																		
f_{53}	0.7131																		
Envs.	1																		
f'_{53}	0.7299																		
γ_1	48°																		
β_1	-73°																		
γ_2	-18°																		
β_2	-39°																		
	<table> <tr><td>Index</td><td>2, 54</td></tr> <tr><td>c_{\max}</td><td>12/13</td></tr> <tr><td>f_{54}</td><td>0.7124</td></tr> <tr><td>Envs.</td><td>2</td></tr> <tr><td>f'_{54}</td><td>0.7296</td></tr> <tr><td>γ_1</td><td>128°</td></tr> <tr><td>β_1</td><td>15°</td></tr> <tr><td>γ_2</td><td>-160°</td></tr> <tr><td>β_2</td><td>36°</td></tr> </table>	Index	2, 54	c_{\max}	12/13	f_{54}	0.7124	Envs.	2	f'_{54}	0.7296	γ_1	128°	β_1	15°	γ_2	-160°	β_2	36°
Index	2, 54																		
c_{\max}	12/13																		
f_{54}	0.7124																		
Envs.	2																		
f'_{54}	0.7296																		
γ_1	128°																		
β_1	15°																		
γ_2	-160°																		
β_2	36°																		
	<table> <tr><td>Index</td><td>2, 55</td></tr> <tr><td>c_{\max}</td><td>12/13</td></tr> <tr><td>f_{55}</td><td>0.7126</td></tr> <tr><td>Envs.</td><td>3</td></tr> <tr><td>f'_{55}</td><td>0.7391</td></tr> <tr><td>γ_1</td><td>38°</td></tr> <tr><td>β_1</td><td>52°</td></tr> <tr><td>γ_2</td><td>108°</td></tr> <tr><td>β_2</td><td>-71°</td></tr> </table>	Index	2, 55	c_{\max}	12/13	f_{55}	0.7126	Envs.	3	f'_{55}	0.7391	γ_1	38°	β_1	52°	γ_2	108°	β_2	-71°
Index	2, 55																		
c_{\max}	12/13																		
f_{55}	0.7126																		
Envs.	3																		
f'_{55}	0.7391																		
γ_1	38°																		
β_1	52°																		
γ_2	108°																		
β_2	-71°																		

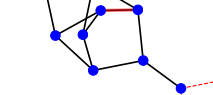
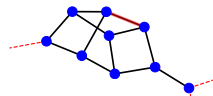
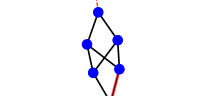
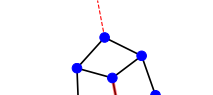
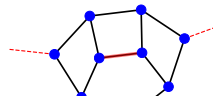
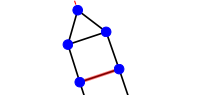

	Index	2, 56
	c_{\max}	11/12
	f_{56}	0.7645
	Envs.	5
	f'_{56}	0.7679
	γ_1	26°
	β_1	59°
	β_2	-17°
	Index	2, 57
	c_{\max}	12/13
	f_{57}	0.7122
	Envs.	1
	f'_{57}	0.7305
	γ_1	-129°
	β_1	-16°
	β_2	52°
	Index	2, 58
	c_{\max}	12/13
	f_{58}	0.7223
	Envs.	11
	f'_{58}	0.7334
	γ_1	-154°
	β_1	27°
	β_2	-13°
	Index	2, 59
	c_{\max}	11/12
	f_{59}	0.7674
	Envs.	16
	f'_{59}	0.7702
	γ_1	-26°
	β_1	-59°
	β_2	17°
	Index	2, 60
	c_{\max}	12/13
	f_{60}	0.7223
	Envs.	7
	f'_{60}	0.7334
	γ_1	-26°
	β_1	28°
	β_2	77°
	Index	2, 61
	c_{\max}	12/13
	f_{61}	0.7178
	Envs.	9
	f'_{61}	0.7325
	γ_1	52°
	β_1	16°
	β_2	37°
	Index	2, 62
	c_{\max}	13/13
	f_{62}	0.7107
	Envs.	1
	f'_{62}	0.7825
	γ_1	-39°
	β_1	-50°
	β_2	-69°

	Index	2, 63
	c_{\max}	11/12
	f_{63}	0.7722
	Envs.	27
	f'_{63}	0.7758
	γ_1	153°
	β_1	-32°
	β_2	-18°
	Index	2, 64
	c_{\max}	11/12
	f_{64}	0.7741
	Envs.	177
	f'_{64}	0.7776
	γ_1	153°
	β_1	-122°
	β_2	108°
	Index	2, 65
	c_{\max}	12/12
	f_{65}	0.7649
	Envs.	10
	f'_{65}	0.7727
	γ_1	206°
	β_1	-57°
	β_2	-133°
	Index	2, 66
	c_{\max}	12/13
	f_{66}	0.7235
	Envs.	24
	f'_{66}	0.7349
	γ_1	51°
	β_1	16°
	β_2	-38°
	Index	2, 67
	c_{\max}	10/12
	f_{67}	0.7784
	Envs.	37
	f'_{67}	0.7794
	γ_1	28°
	β_1	58°
	β_2	-18°
	Index	2, 68
	c_{\max}	11/11
	f_{68}	0.8153
	Envs.	90
	f'_{68}	0.8347
	γ_1	150°
	β_1	55°
	β_2	-22°
	Index	2, 69
	c_{\max}	10/12
	f_{69}	0.7775
	Envs.	39
	f'_{69}	0.7786
	γ_1	152°
	β_1	-32°
	β_2	-49°

	Index	2, 70
	c_{\max}	11/12
	f_{70}	0.77799
	Envs.	136
	f'_{70}	0.7811
	γ_1	-208°
	β_1	58°
	γ_2	130°
	β_2	108°
	Index	2, 71
	c_{\max}	11/11
	f_{71}	0.8181
	Envs.	576
	f'_{71}	0.8346
	γ_1	29°
	β_1	-35°
	γ_2	49°
	β_2	-21°
	Index	2, 72
	c_{\max}	11/12
	f_{72}	0.7818
	Envs.	127
	f'_{72}	0.7834
	γ_1	151°
	β_1	-32°
	γ_2	130°
	β_2	18°
	Index	2, 73
	c_{\max}	12/13
	f_{73}	0.7316
	Envs.	12
	f'_{73}	0.7399
	γ_1	27°
	β_1	62°
	γ_2	-130°
	β_2	-77°
	Index	2, 74
	c_{\max}	12/13
	f_{74}	0.7324
	Envs.	19
	f'_{74}	0.7403
	γ_1	-28°
	β_1	28°
	γ_2	130°
	β_2	77°
	Index	2, 75
	c_{\max}	7/8
	f_{75}	0.7559
	Envs.	5
	f'_{75}	0.7960
	γ_1	142°
	β_1	-30°
	γ_2	127°
	β_2	25°
	Index	2, 76
	c_{\max}	7/9
	f_{76}	0.6522
	Envs.	1
	f'_{76}	0.6660
	γ_1	-158°
	β_1	25°
	γ_2	46°
	β_2	-78°

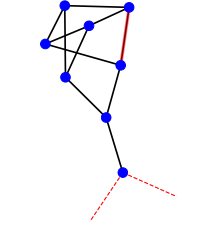
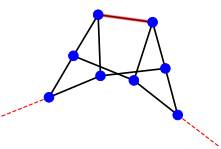
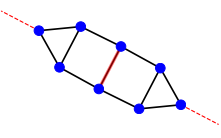
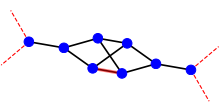
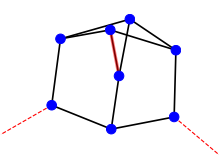
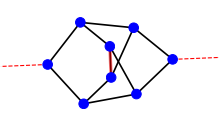
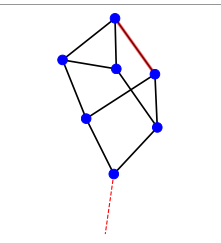
	Index	2, 77
	c_{\max}	10/12
	f_{77}	0.7552
	Envs.	2
	f'_{77}	0.7674
	γ_1	208°
	β_1	-64°
	γ_2	52°
	β_2	14°
	Index	2, 78
	c_{\max}	9/11
	f_{78}	0.8105
	Envs.	1
	f'_{78}	0.8395
	γ_1	-147°
	β_1	-65°
	γ_2	242°
	β_2	-16°
	Index	2, 79
	c_{\max}	11/12
	f_{79}	0.7579
	Envs.	1
	f'_{79}	0.7657
	γ_1	-153°
	β_1	-63°
	γ_2	50°
	β_2	15°
	Index	2, 80
	c_{\max}	10/11
	f_{80}	0.8185
	Envs.	8
	f'_{80}	0.8261
	γ_1	-148°
	β_1	-60°
	γ_2	55°
	β_2	18°
	Index	2, 81
	c_{\max}	10/11
	f_{81}	0.8207
	Envs.	44
	f'_{81}	0.8302
	γ_1	-32°
	β_1	120°
	γ_2	-236°
	β_2	72°
	Index	2, 82
	c_{\max}	10/11
	f_{82}	0.8154
	Envs.	5
	f'_{82}	0.8213
	γ_1	-31°
	β_1	-59°
	γ_2	-53°
	β_2	19°
	Index	2, 83
	c_{\max}	10/12
	f_{83}	0.7621
	Envs.	2
	f'_{83}	0.7797
	γ_1	-148°
	β_1	26°
	γ_2	-122°
	β_2	-14°

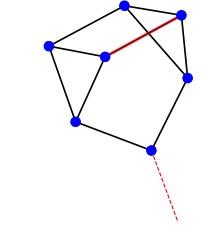
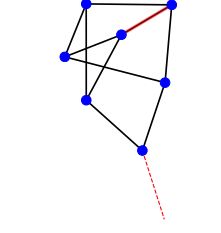
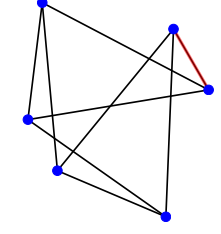
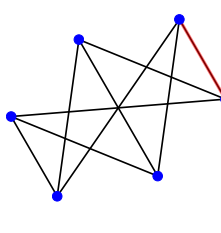
	Index 2, 84 c_{\max} 11/12 f_{84} 0.7605 Envs. 1 f'_{84} 0.7726 γ_1 -149° β_1 -63° γ_2 -126° β_2 -105°
	Index 2, 85 c_{\max} 10/12 f_{85} 0.7694 Envs. 10 f'_{85} 0.7831 γ_1 -32° β_1 27° γ_2 -57° β_2 15°
	Index 2, 86 c_{\max} 9/11 f_{86} 0.8147 Envs. 5 f'_{86} 0.8584 γ_1 -35° β_1 -66° γ_2 113° β_2 74°
	Index 2, 87 c_{\max} 12/13 f_{87} 0.7024 Envs. 1 f'_{87} 0.7339 γ_1 -142° β_1 -51° γ_2 107° β_2 -19°
	Index 2, 88 c_{\max} 10/12 f_{88} 0.7604 Envs. 6 f'_{88} 0.7639 γ_1 -26° β_1 -59° γ_2 133° β_2 -17°
	Index 2, 89 c_{\max} 12/13 f_{89} 0.7067 Envs. 1 f'_{89} 0.7282 γ_1 54° β_1 14° γ_2 -21° β_2 55°
	Index 2, 90 c_{\max} 11/12 f_{90} 0.7639 Envs. 6 f'_{90} 0.7663 γ_1 -153° β_1 31° γ_2 48° β_2 17°

	Index 2, 91 c_{\max} 10/12 f_{91} 0.7615 Envs. 2 f'_{91} 0.7647 γ_1 154° β_1 -31° γ_2 133° β_2 17°
	Index 2, 92 c_{\max} 11/12 f_{92} 0.7556 Envs. 2 f'_{92} 0.7620 γ_1 25° β_1 59° γ_2 -134° β_2 18°
	Index 2, 93 c_{\max} 11/11 f_{93} 0.8017 Envs. 5 f'_{93} 0.8208 γ_1 -152° β_1 -56° γ_2 47° β_2 22°
	Index 2, 94 c_{\max} 11/11 f_{94} 0.8041 Envs. 44 f'_{94} 0.8203 γ_1 -27° β_1 35° γ_2 132° β_2 -21°
	Index 2, 95 c_{\max} 11/12 f_{95} 0.7617 Envs. 10 f'_{95} 0.7679 γ_1 26° β_1 -32° γ_2 -134° β_2 18°
	Index 2, 96 c_{\max} 10/11 f_{96} 0.8127 Envs. 35 f'_{96} 0.8235 γ_1 -152° β_1 -56° γ_2 229° β_2 -110°
	Index 2, 97 c_{\max} 10/12 f_{97} 0.7738 Envs. 5 f'_{97} 0.7745 γ_1 -152° β_1 -59° γ_2 -131° β_2 -17°

	Index	2, 98
	c_{\max}	10/11
	f_{98}	0.8109
	Envs.	33
	f'_{98}	0.8256
	γ_1	-29°
	β_1	34°
	γ_2	132°
	β_2	69°
	Index	2, 99
	c_{\max}	10/12
	f_{99}	0.7734
	Envs.	10
	f'_{99}	0.7742
	γ_1	28°
	β_1	-31°
	γ_2	-131°
	β_2	107°
	Index	2, 100
	c_{\max}	10/11
	f_{100}	0.8112
	Envs.	39
	f'_{100}	0.8220
	γ_1	-28°
	β_1	34°
	γ_2	-49°
	β_2	-70°
	Index	2, 101
	c_{\max}	9/11
	f_{101}	0.7943
	Envs.	1
	f'_{101}	0.8324
	γ_1	147°
	β_1	66°
	γ_2	115°
	β_2	-74°
	Index	2, 102
	c_{\max}	9/11
	f_{102}	0.7976
	Envs.	1
	f'_{102}	0.8200
	γ_1	-149°
	β_1	-65°
	γ_2	59°
	β_2	16°
	Index	2, 103
	c_{\max}	9/10
	f_{103}	0.8452
	Envs.	5
	f'_{103}	0.8548
	γ_1	-30°
	β_1	-59°
	γ_2	-51°
	β_2	20°
	Index	2, 104
	c_{\max}	10/11
	f_{104}	0.8026
	Envs.	1
	f'_{104}	0.8094
	γ_1	-31°
	β_1	29°
	γ_2	-53°
	β_2	17°

	Index	2, 105
	c_{\max}	9/10
	f_{105}	0.8522
	Envs.	18
	f'_{105}	0.8608
	γ_1	-31°
	β_1	32°
	γ_2	-53°
	β_2	20°
	Index	2, 106
	c_{\max}	10/11
	f_{106}	0.8108
	Envs.	4
	f'_{106}	0.8177
	γ_1	32°
	β_1	-30°
	γ_2	54°
	β_2	72°
	Index	2, 107
	c_{\max}	8/10
	f_{107}	0.8545
	Envs.	1
	f'_{107}	0.8828
	γ_1	214°
	β_1	-62°
	γ_2	-119°
	β_2	-18°
	Index	2, 108
	c_{\max}	10/12
	f_{108}	0.7473
	Envs.	1
	f'_{108}	0.7669
	γ_1	148°
	β_1	-115°
	γ_2	124°
	β_2	14°
	Index	2, 109
	c_{\max}	9/11
	f_{109}	0.8061
	Envs.	3
	f'_{109}	0.8538
	γ_1	35°
	β_1	67°
	γ_2	68°
	β_2	74°
	Index	2, 110
	c_{\max}	10/11
	f_{110}	0.7917
	Envs.	5
	f'_{110}	0.8011
	γ_1	-26°
	β_1	33°
	γ_2	133°
	β_2	-19°
	Index	2, 111
	c_{\max}	10/12
	f_{111}	0.7461
	Envs.	1
	f'_{111}	0.7541
	γ_1	-25°
	β_1	-61°
	γ_2	-45°
	β_2	16°

	<table> <tr><td>Index</td><td>2, 112</td></tr> <tr><td>c_{\max}</td><td>10/11</td></tr> <tr><td>f_{112}</td><td>0.7930</td></tr> <tr><td>Envs.</td><td>1</td></tr> <tr><td>f'_{112}</td><td>0.8051</td></tr> <tr><td>γ_1</td><td>152°</td></tr> <tr><td>β_1</td><td>-33°</td></tr> <tr><td>γ_2</td><td>-46°</td></tr> <tr><td>β_2</td><td>-20°</td></tr> </table>	Index	2, 112	c_{\max}	10/11	f_{112}	0.7930	Envs.	1	f'_{112}	0.8051	γ_1	152°	β_1	-33°	γ_2	-46°	β_2	-20°
Index	2, 112																		
c_{\max}	10/11																		
f_{112}	0.7930																		
Envs.	1																		
f'_{112}	0.8051																		
γ_1	152°																		
β_1	-33°																		
γ_2	-46°																		
β_2	-20°																		
	<table> <tr><td>Index</td><td>2, 113</td></tr> <tr><td>c_{\max}</td><td>11/11</td></tr> <tr><td>f_{113}</td><td>0.7895</td></tr> <tr><td>Envs.</td><td>3</td></tr> <tr><td>f'_{113}</td><td>0.8079</td></tr> <tr><td>γ_1</td><td>-154°</td></tr> <tr><td>β_1</td><td>34°</td></tr> <tr><td>γ_2</td><td>-134°</td></tr> <tr><td>β_2</td><td>-21°</td></tr> </table>	Index	2, 113	c_{\max}	11/11	f_{113}	0.7895	Envs.	3	f'_{113}	0.8079	γ_1	-154°	β_1	34°	γ_2	-134°	β_2	-21°
Index	2, 113																		
c_{\max}	11/11																		
f_{113}	0.7895																		
Envs.	3																		
f'_{113}	0.8079																		
γ_1	-154°																		
β_1	34°																		
γ_2	-134°																		
β_2	-21°																		
	<table> <tr><td>Index</td><td>2, 114</td></tr> <tr><td>c_{\max}</td><td>9/11</td></tr> <tr><td>f_{114}</td><td>0.8068</td></tr> <tr><td>Envs.</td><td>2</td></tr> <tr><td>f'_{114}</td><td>0.8136</td></tr> <tr><td>γ_1</td><td>28°</td></tr> <tr><td>β_1</td><td>-33°</td></tr> <tr><td>γ_2</td><td>-132°</td></tr> <tr><td>β_2</td><td>20°</td></tr> </table>	Index	2, 114	c_{\max}	9/11	f_{114}	0.8068	Envs.	2	f'_{114}	0.8136	γ_1	28°	β_1	-33°	γ_2	-132°	β_2	20°
Index	2, 114																		
c_{\max}	9/11																		
f_{114}	0.8068																		
Envs.	2																		
f'_{114}	0.8136																		
γ_1	28°																		
β_1	-33°																		
γ_2	-132°																		
β_2	20°																		
	<table> <tr><td>Index</td><td>2, 115</td></tr> <tr><td>c_{\max}</td><td>10/10</td></tr> <tr><td>f_{115}</td><td>0.8316</td></tr> <tr><td>Envs.</td><td>15</td></tr> <tr><td>f'_{115}</td><td>0.8667</td></tr> <tr><td>γ_1</td><td>-29°</td></tr> <tr><td>β_1</td><td>35°</td></tr> <tr><td>γ_2</td><td>134°</td></tr> <tr><td>β_2</td><td>-23°</td></tr> </table>	Index	2, 115	c_{\max}	10/10	f_{115}	0.8316	Envs.	15	f'_{115}	0.8667	γ_1	-29°	β_1	35°	γ_2	134°	β_2	-23°
Index	2, 115																		
c_{\max}	10/10																		
f_{115}	0.8316																		
Envs.	15																		
f'_{115}	0.8667																		
γ_1	-29°																		
β_1	35°																		
γ_2	134°																		
β_2	-23°																		
	<table> <tr><td>Index</td><td>2, 116</td></tr> <tr><td>c_{\max}</td><td>10/11</td></tr> <tr><td>f_{116}</td><td>0.8068</td></tr> <tr><td>Envs.</td><td>4</td></tr> <tr><td>f'_{116}</td><td>0.8179</td></tr> <tr><td>γ_1</td><td>-151°</td></tr> <tr><td>β_1</td><td>-57°</td></tr> <tr><td>γ_2</td><td>-132°</td></tr> <tr><td>β_2</td><td>-110°</td></tr> </table>	Index	2, 116	c_{\max}	10/11	f_{116}	0.8068	Envs.	4	f'_{116}	0.8179	γ_1	-151°	β_1	-57°	γ_2	-132°	β_2	-110°
Index	2, 116																		
c_{\max}	10/11																		
f_{116}	0.8068																		
Envs.	4																		
f'_{116}	0.8179																		
γ_1	-151°																		
β_1	-57°																		
γ_2	-132°																		
β_2	-110°																		
	<table> <tr><td>Index</td><td>2, 117</td></tr> <tr><td>c_{\max}</td><td>9/11</td></tr> <tr><td>f_{117}</td><td>0.8038</td></tr> <tr><td>Envs.</td><td>3</td></tr> <tr><td>f'_{117}</td><td>0.8111</td></tr> <tr><td>γ_1</td><td>-153°</td></tr> <tr><td>β_1</td><td>-57°</td></tr> <tr><td>γ_2</td><td>-132°</td></tr> <tr><td>β_2</td><td>70°</td></tr> </table>	Index	2, 117	c_{\max}	9/11	f_{117}	0.8038	Envs.	3	f'_{117}	0.8111	γ_1	-153°	β_1	-57°	γ_2	-132°	β_2	70°
Index	2, 117																		
c_{\max}	9/11																		
f_{117}	0.8038																		
Envs.	3																		
f'_{117}	0.8111																		
γ_1	-153°																		
β_1	-57°																		
γ_2	-132°																		
β_2	70°																		
	<table> <tr><td>Index</td><td>2, 118</td></tr> <tr><td>c_{\max}</td><td>9/10</td></tr> <tr><td>f_{118}</td><td>0.8407</td></tr> <tr><td>Envs.</td><td>1</td></tr> <tr><td>f'_{118}</td><td>0.8475</td></tr> <tr><td>γ_1</td><td>150°</td></tr> <tr><td>β_1</td><td>58°</td></tr> <tr><td>γ_2</td><td>-51°</td></tr> <tr><td>β_2</td><td>-20°</td></tr> </table>	Index	2, 118	c_{\max}	9/10	f_{118}	0.8407	Envs.	1	f'_{118}	0.8475	γ_1	150°	β_1	58°	γ_2	-51°	β_2	-20°
Index	2, 118																		
c_{\max}	9/10																		
f_{118}	0.8407																		
Envs.	1																		
f'_{118}	0.8475																		
γ_1	150°																		
β_1	58°																		
γ_2	-51°																		
β_2	-20°																		

	<table> <tr><td>Index</td><td>2, 119</td></tr> <tr><td>c_{\max}</td><td>8/10</td></tr> <tr><td>f_{119}</td><td>0.8480</td></tr> <tr><td>Envs.</td><td>1</td></tr> <tr><td>f'_{119}</td><td>0.8799</td></tr> <tr><td>γ_1</td><td>35°</td></tr> <tr><td>β_1</td><td>-27°</td></tr> <tr><td>γ_2</td><td>62°</td></tr> <tr><td>β_2</td><td>73°</td></tr> </table>	Index	2, 119	c_{\max}	8/10	f_{119}	0.8480	Envs.	1	f'_{119}	0.8799	γ_1	35°	β_1	-27°	γ_2	62°	β_2	73°
Index	2, 119																		
c_{\max}	8/10																		
f_{119}	0.8480																		
Envs.	1																		
f'_{119}	0.8799																		
γ_1	35°																		
β_1	-27°																		
γ_2	62°																		
β_2	73°																		
	<table> <tr><td>Index</td><td>2, 120</td></tr> <tr><td>c_{\max}</td><td>9/10</td></tr> <tr><td>f_{120}</td><td>0.8270</td></tr> <tr><td>Envs.</td><td>1</td></tr> <tr><td>f'_{120}</td><td>0.8566</td></tr> <tr><td>γ_1</td><td>151°</td></tr> <tr><td>β_1</td><td>56°</td></tr> <tr><td>γ_2</td><td>134°</td></tr> <tr><td>β_2</td><td>22°</td></tr> </table>	Index	2, 120	c_{\max}	9/10	f_{120}	0.8270	Envs.	1	f'_{120}	0.8566	γ_1	151°	β_1	56°	γ_2	134°	β_2	22°
Index	2, 120																		
c_{\max}	9/10																		
f_{120}	0.8270																		
Envs.	1																		
f'_{120}	0.8566																		
γ_1	151°																		
β_1	56°																		
γ_2	134°																		
β_2	22°																		
	<table> <tr><td>Index</td><td>2, 121</td></tr> <tr><td>c_{\max}</td><td>7/9</td></tr> <tr><td>f_{121}</td><td>0.8771</td></tr> <tr><td>Envs.</td><td>1</td></tr> <tr><td>f'_{121}</td><td>0.8935</td></tr> <tr><td>γ_1</td><td>-32°</td></tr> <tr><td>β_1</td><td>-61°</td></tr> <tr><td>γ_2</td><td>-57°</td></tr> <tr><td>β_2</td><td>108°</td></tr> </table>	Index	2, 121	c_{\max}	7/9	f_{121}	0.8771	Envs.	1	f'_{121}	0.8935	γ_1	-32°	β_1	-61°	γ_2	-57°	β_2	108°
Index	2, 121																		
c_{\max}	7/9																		
f_{121}	0.8771																		
Envs.	1																		
f'_{121}	0.8935																		
γ_1	-32°																		
β_1	-61°																		
γ_2	-57°																		
β_2	108°																		
	<table> <tr><td>Index</td><td>2, 122</td></tr> <tr><td>c_{\max}</td><td>9/9</td></tr> <tr><td>f_{122}</td><td>0.8340</td></tr> <tr><td>Envs.</td><td>1</td></tr> <tr><td>f'_{122}</td><td>0.8911</td></tr> <tr><td>γ_1</td><td>-28°</td></tr> <tr><td>β_1</td><td>-55°</td></tr> <tr><td>γ_2</td><td>-44°</td></tr> <tr><td>β_2</td><td>-66°</td></tr> </table>	Index	2, 122	c_{\max}	9/9	f_{122}	0.8340	Envs.	1	f'_{122}	0.8911	γ_1	-28°	β_1	-55°	γ_2	-44°	β_2	-66°
Index	2, 122																		
c_{\max}	9/9																		
f_{122}	0.8340																		
Envs.	1																		
f'_{122}	0.8911																		
γ_1	-28°																		
β_1	-55°																		
γ_2	-44°																		
β_2	-66°																		